Neoproterozoic-hosted Carlin-type mineralization in central Yukon, part 2: Mineralization

Nicolas Pinet[1*], Patrick Sack[2], Patrick Mercier-Langevin[1], William J. Davis[3], Denis Lavoie[1], Omid Haeri-Ardakani[4], Bram A. Komaromi[4], Benoît Dubé[1], Jean S. Cline[5], Duane C. Petts[3], Josué Jautzy[1], Simon E. Jackson[3], Jeanne B. Percival[3], Martine M. Savard[1], and Virginia I. Brake[1]

[1]Geological Survey of Canada, 490 rue de la Couronne, Québec, Quebec G1K 9A9
[2]Yukon Geological Survey, 91807 Alaska Hwy, Whitehorse, Yukon Y1A 5B7
[3]Geological Survey of Canada, 601 Booth Street, Ottawa, Ontario K1A 0E9
[4]Geological Survey of Canada, 3303 33rd Street NW, Calgary, Alberta T2L 2A7
[5]University of Nevada, 4505 South Maryland Parkway, Las Vegas, Nevada 89154-4010
*Corresponding author's e-mail: nicolas.pinet@canada.ca

ABSTRACT

Gold-rich zones in the Nadaleen trend (central Yukon) exhibit several characteristics consistent with Carlin-type mineralization: 1) alteration zones with partial to complete decalcification of mineralized intervals and very fine-grained quartz associated with silicification; 2) the association of gold with certain pathfinder elements (Tl, As, Hg, and Sb) and minerals (realgar, orpiment, and fluorite); 3) the low base metal and Ag content of the mineralized intervals; and 4) the 'invisible' nature of gold, which occurs as rims of Au-bearing arsenian pyrite on pre-ore pyrite and/or as sub-micrometre particles. Mineralization styles vary significantly between intervals and even within an interval, attesting to the 'passive' or 'opportunistic' nature of the mineralizing fluids that exploited a variety of porous and permeable pathways regardless of their sedimentary and/or tectonic origin. Alternating finely laminated limestone and siltstone (Conrad zone) and floatstone intervals (Conrad, Sunrise, and Osiris zones) are the most favourable sedimentary units. Pre-mineralization fractures acted as feeders for selective bed replacement and pre-mineralization vein networks were preferentially dissolved by early acidic fluids and channelized later by gold-bearing fluids. With ongoing research, we hope to better constrain the occurrence of gold at the micron scale, the geochemical variations due to alteration, the temperature of the mineralizing fluids, and the timing of the gold mineralization.

INTRODUCTION

Carlin-type gold systems are the results of a number of critical geological processes acting at lithospheric to mineral scales (Cline et al., 2005; Muntean, 2018). The regional- to prospect-scale setting of Carlin-type gold zones in central Yukon (Nadaleen trend, Fig. 1) has been reviewed by Pinet et al. (2020). These zones are located close to the northern boundary of the Selwyn Basin, a domain characterized by sedimentary rocks deposited in deeper water settings than surrounding domains. The northern boundary of the basin is controlled by the Dawson fault, a long-lived deep-seated structure. In the Nadaleen trend, the sedimentary succession is Neoproterozoic to early Permian and includes fine- to coarse-grained clastic and carbonate rocks. The structural style of the Nadaleen trend is complex; strata generally dip steeper than in classical fold-and-thrust belts and faults include a significant component of strike-slip motion. Carlin-type mineralized zones are mainly hosted in two Neoproterozoic limestone units (informally known as the Conrad and Osiris limestones, and formally referred to as the Nadaleen and Gametrail formations, respectively; Moynihan et al., 2019) and in variably calcareous Paleozoic siltstone. In Neoproterozoic-hosted zones, mineralized intervals are grossly concordant with bedding in complexly shaped anticlines. This contribution complements Pinet et al. (2020) and focuses mainly on Neoproterozoic-hosted mineralized zones at the tens of metres to thin-section scale.

MINERALIZATION

History of Exploration

The Nadaleen trend was discovered in 2010 by ATAC Resources Ltd. during a follow-up investigation of arsenic anomalies detected in a regional stream sediment sampling program conducted by the Geological Survey of Canada (Goodfellow and Lynch, 1978). Subsequent analysis of arsenic in soil was a highly successful exploration tool with all known gold mineralization occurrences being spatially associated with a multi-element soil anomaly.

Pinet, N., Sack, P., Mercier-Langevin, P., Davis, W.J., Lavoie, D., Haeri-Ardakani, O., Komaromi, B.A., Dubé, B., Cline, J.S., Petts, D.C., Jautzy, J., Jackson, S.E., Percival. J.B., Savard, M.M., and Brake, V.I., 2020. Neoproterozoic-hosted Carlin-type mineralization in central Yukon part 2: Mineralization; *in* Targeted Geoscience Initiative 5: Contributions to the Understanding of Canadian Gold Systems, (ed.) P. Mercier-Langevin, C.J.M. Lawley, and S. Castonguay; Geological Survey of Canada, Open File 8712, p. 299–314. https://doi.org/10.4095/326047

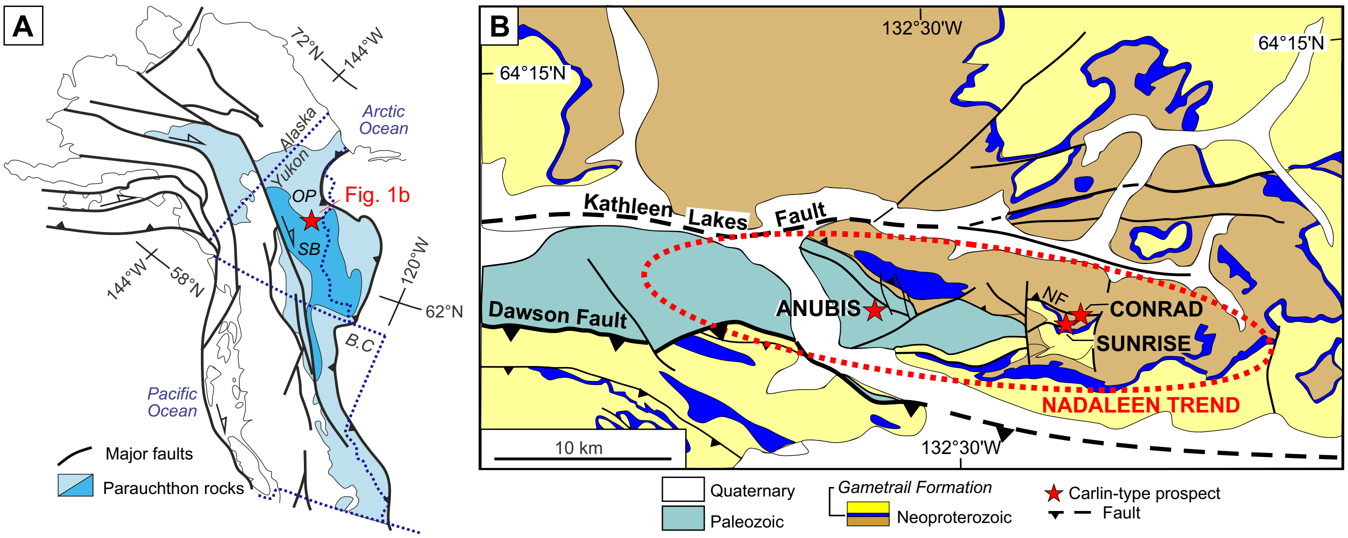

Figure 1. Geological map of the Nadaleen trend (*modified from* Moynihan, 2016). Abbreviations: B.C. = British Columbia, NF = Nadaleen fault, OP = Olgilvie Platform, SB = Selwyn Basin.

Drill targeting of the realgar-rich mineralized zones, which are locally exposed at surface, started in 2010. To date, more than 90 kms of drilling have been completed in five main zones. In June 2018, the first gold resource estimate for the Neoproterozoic-hosted Osiris cluster (Conrad, Ibis, Osiris, and Sunrise zones) was published by ATAC Resources at 8 Mt at 4.1 g/t amenable to open pit mining and 4.3 Mt at 4.52 g/t amenable to underground mining, for a total of about 1.7 Moz (52.3 metric t) (Ristorcelli et al., 2018). All gold-bearing zones have significant potential for additional resources, both along-strike and at depth.

Common Characteristics of Mineralization

Realgar and orpiment±fluorite are generally good visual guides for gold mineralization in Neoproterozoic-hosted Carlin-type mineralized zones. In some cases, realgar is found in calcite veins that clearly post-date the main stage of gold mineralization. However, the spatial association of realgar and orpiment with gold-rich intervals indicates that these minerals formed during the late stage of a single event, not during a later hydrothermal pulse unrelated to gold mineralization (Pinet et al., 2018; Tucker et al. 2018; Pinet and Sack, 2019).

At the macroscopic scale, mineralized zone contacts are generally sharp. Decalcification is the main alteration type associated with gold mineralization and resulted in a significant increase in the porosity of the host rocks. The intensity of decalcification varies strongly, with some decimetre-scale intervals reacting with HCl a few centimetres from totally decalcified mineralized segments. Silicification and argillization are more subtle to document visually, but may be significant alteration styles at the microscopic scale, as described below.

First-Order Lithological and Structural Controls on Mineralization

In the Conrad, Sunrise, and Osiris mineralized zones (Fig. 1), the geometry of the sedimentary units with permeability either higher or lower than the surrounding rocks exerted a first-order control on gold-bearing fluid flow (Pinet and Sack, 2019; Pinet et al., 2020). Figure 2 shows two nearly perpendicular sections of the Conrad zone and illustrates the tight domal geometry of the limestone unit. This geometry constitutes a four-way, dip-closure fold/fault trap for mineralizing fluids (Pinet et al., 2020). The mixed stratigraphic-structural trap is sealed by two low-permeability mudstone/siltstone units: the NONAD mudstone (Ice Brook Formation) that is in fault contact with the Conrad limestone to the north and the Conrad siliciclastic rocks (Nadaleen Formation) that stratigraphically overlie the limestone to the south. These siliciclastic units (including the Nadaleen fault damage zone) acted as prospect-scale aquitards. At the tens of metre scale, some relatively thick (>1 m) massive, and weakly fractured limestone beds also may have acted as discontinuous impermeable barriers. In the Conrad zone, gold mineralized bodies are mainly hosted in three settings (Fig. 3): 1) the steeply dipping upper part of the limestone unit, close to its contact with stratigraphically overlying siliciclastic rocks; 2) in fractured corridors associated with the north-northwest-trending faults, including the 350 and 850 faults; and 3) in the immediate footwall of the Nadaleen fault. Due to the closure of the main host units at the top of the Conrad limestone, and to increased fracture density in the hinge zone, the mineralization envelope is more continuous in map view close to surface (Fig. 3).

In the Sunrise and Osiris zones (Fig. 4), the location of the steeply dipping limestone host unit (Osiris lime-

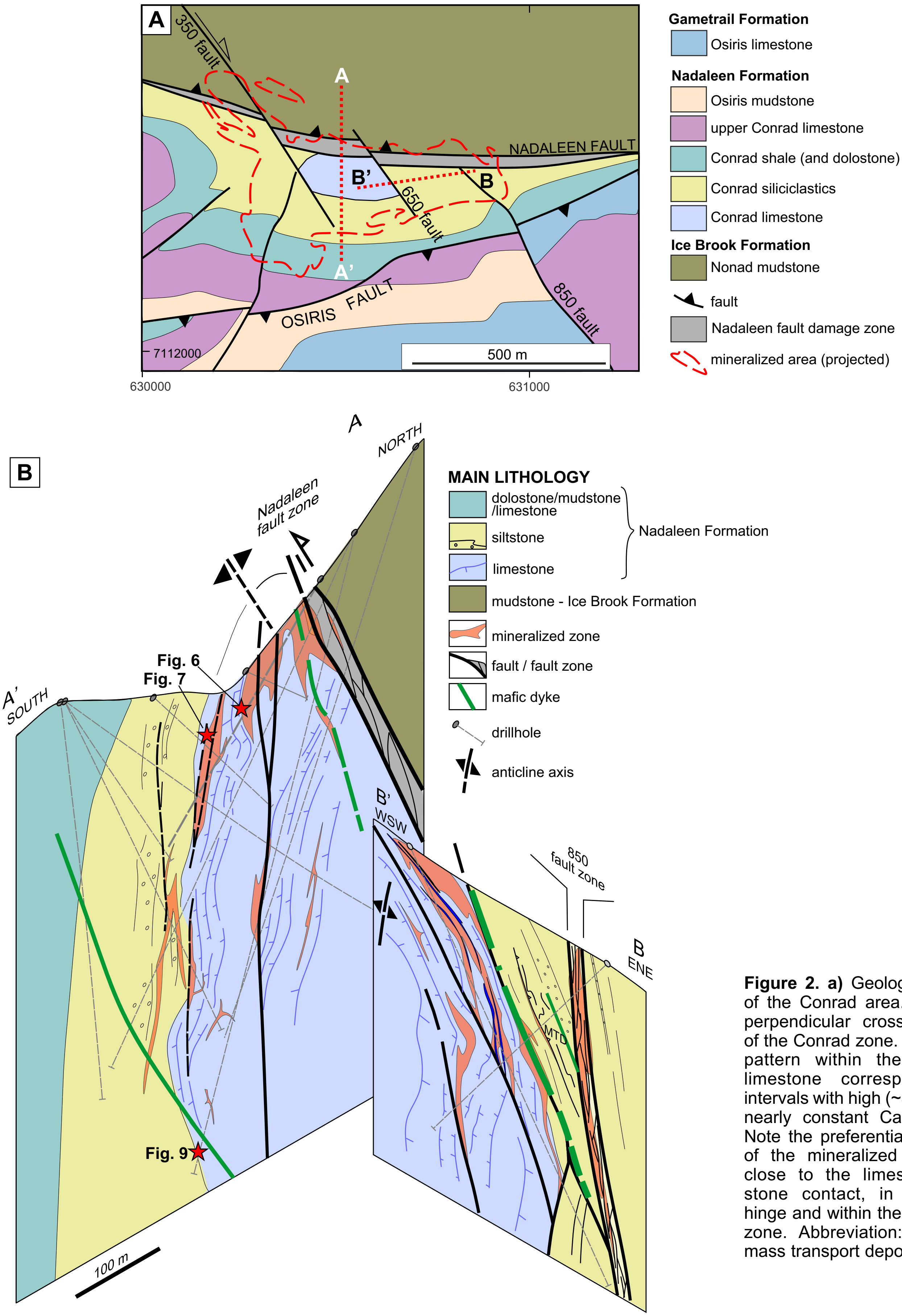

Figure 2. a) Geological map of the Conrad area. **b)** Sub-perpendicular cross-sections of the Conrad zone. The brick pattern within the Conrad limestone corresponds to intervals with high (~34%) and nearly constant Ca content. Note the preferential location of the mineralized intervals close to the limestone-siltstone contact, in the fold hinge and within the 850 fault zone. Abbreviation: MTD = mass transport deposit.

stone of the Gametrail Formation) between low-permeability intervals (Osiris mudstone and Osiris fault zone in the Sunrise area; Osiris mudstone and Osiris dolostone in the Osiris area) is a first-order control on fluid flow. At the scale of tens of metres, the location of the mineralized bodies in the Sunrise and Osiris zones were also controlled by tight, clast-supported rudstone intervals (flat-pebble conglomerate with lime mudstone fragments showing indented and stylolitic relationships) that are found in the Osiris limestone. These rudstone intervals acted as local discontinuous impermeable barriers (Pinet and Sack, 2019).

Second-Order Sedimentological and Structural Controls on Mineralization

Drill core indicates that sedimentological and structural parameters provided second-order controls that resulted in a complex geometry of gold zones and variable mineralization styles and breccia types. As documented in Pinet et al. (2018) and Pinet and Sack (2019), sedimentological and structural controls are not mutually exclusive and multiple mineralization styles are documented in the same interval.

Sedimentological control

At the macroscopic scale, several mineralization styles denote a predominant sedimentological control.

1. Selective replacement of beds. This mineralization style is documented in all Neoproterozoic-hosted mineralized zones and is mainly restricted to intervals including millimetre to centimetre thick limestone beds with a granular texture alternating with millimetre thick fine-grained beds (Fig. 5a). Drill core indicates that mineralized beds are connected to feeder veins at high angles to bedding (Fig. 5b). In a few cases, mineralization is confined to mudstone beds bounded by massive limestone beds (Fig. 5c).
2. Mineralized floatstone (debris flow). Matrix-supported, monomictic to polymictic, floatstone intervals are the most favourable host-rocks for gold mineralization at the Sunrise and Osiris zones (Fig. 5e,f; Pinet and Sack, 2019). Floatstone-hosted mineralization also represents a significant part of high-grade (>5 g/t Au) intervals in the Conrad zone (Fig. 5d, 6). Clasts are generally calcareous (lime mudstone to packstone with variable colours and laminations), represent between 40 and 90 vol.% of the rock, are angular to subangular, and show no clear preferential orientation, except close to the basal contact. Mineralization is confined to the generally silty matrix and to a few fractures within clasts. Realgar is ubiquitous in mineralized floatstone intervals within the Osiris limestone of the Gametrail Formation (Osiris, Sunrise, and Ibis

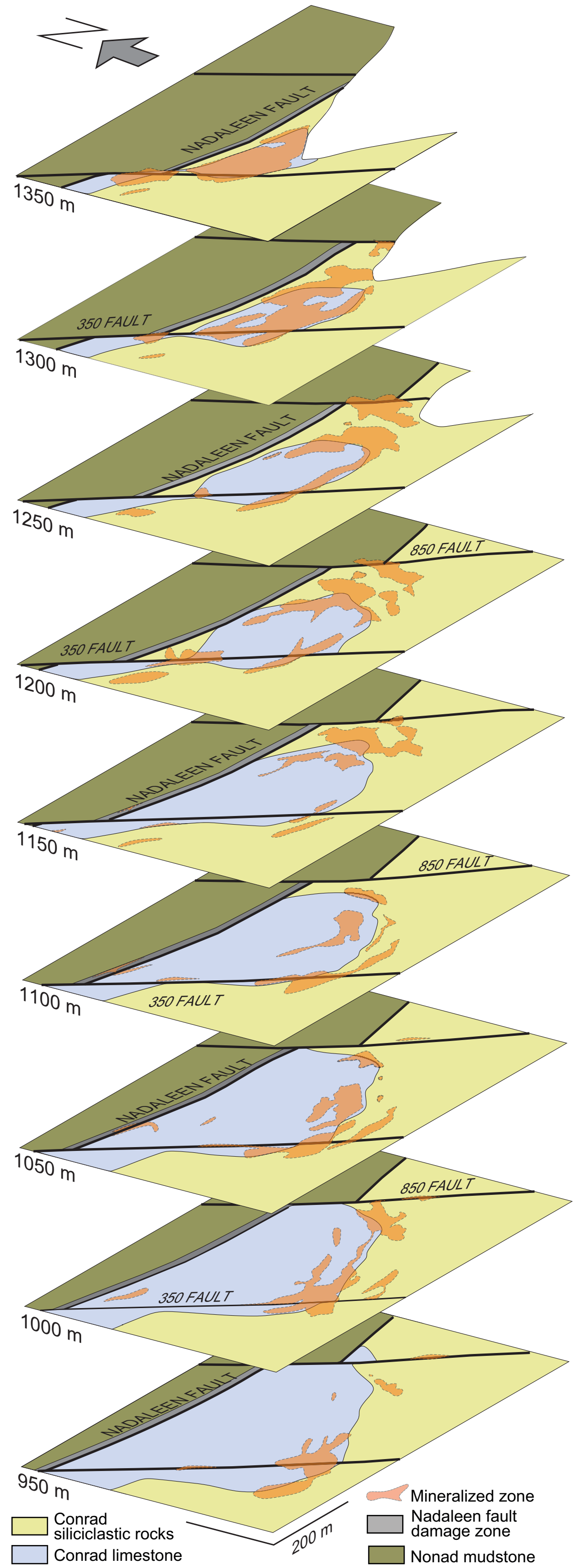

Figure 3. Map views of the Conrad zone showing the location of mineralized zones at several elevations. Same colour scheme as used in Figure 2. Note the preferential location of the mineralized intervals close to the limestone-siltstone contact, in the fold hinge (1300–1350 m elevation), and within/close to the 350 and 850 fault zones.

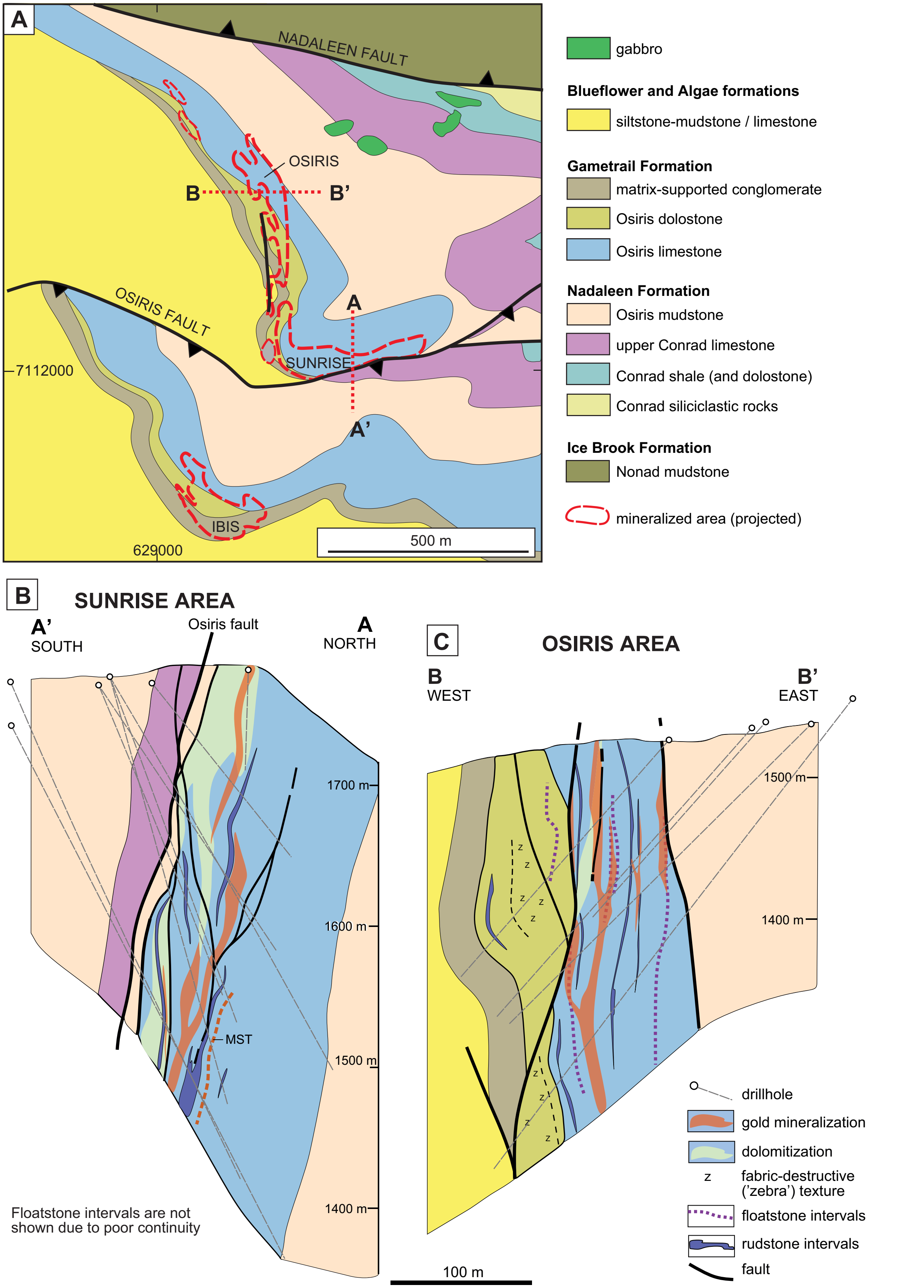

Figure 4. a) Geological map of the Osiris-Sunrise-Ibis area. **b and c)** Cross-sections of the Sunrise and Osiris gold-bearing zones, respectively. Note that mineralized intervals are mostly concordant with bedding. Abbreviation: MST = mudstone.

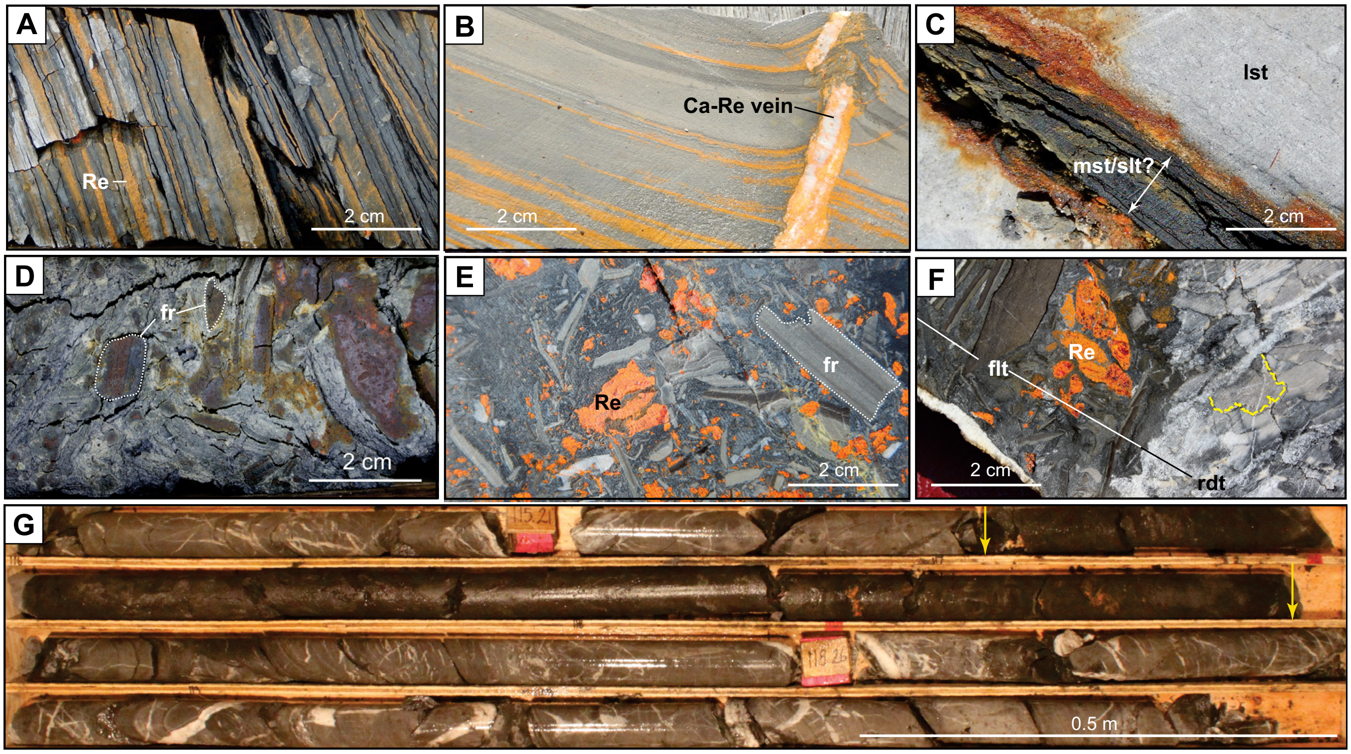

Figure 5. Photographs illustrating the sedimentological control on mineralization. Photographs (a), (b), (d), and (g) are from the Conrad zone. Photographs (b),(e), and (f) are from the Sunrise zone. **a)** Finely laminated limestone showing the selective replacement of 1–5 mm thick beds with realgar (Re). **b)** Selective replacement of 1–4 mm thick beds and bedding-perpendicular calcite-realgar feeder vein (Ca-Re vein). **c)** Mineralized fine-grained bed (originally calcareous mudstone/siltstone?: mst/slt?) bounded by barren thickly bedded massive limestones (lst). **d)** Mineralized floatstone interval with monomictic fragments (fr). **e)** Mineralized floatstone interval with angular fragments (fr) of various orientation. Note that realgar (Re) is found exclusively in the matrix. **f)** Contact between a mineralized matrix-supported floatstone (flt) and a barren clast-supported rudstone (rdt). Note the stylolitic relationship between the fragments (yellow dashed line) in the rudstone. **g)** A 1.82 m thick black, almost featureless decarbonatized interval (between the yellow arrows) yielding 9.88 g/t Au.

zones), but is rarely present within the Conrad limestone of the Nadaleen Formation (Conrad zone).

3. Dark grey to black mineralized interval. These decimetre to metre thick decarbonatized intervals (Fig. 5g) are visually featureless with only a few laminations preserved locally. Their boundaries are concordant with bedding and a few irregularly shaped fragments are observed, suggesting that these intervals were originally matrix-rich, floatstone intervals.

In the Conrad zone, all of the mineralization styles described above are developed in the upper part of the limestone unit that hosts a significant portion of the mineralization (Fig. 3). Figure 7 illustrates a high-grade mineralized interval located close to the limestone-siltstone contact that consists of interbedded and thinly bedded, lime mudstone, packstone, floatstone, and calcareous siltstone. In this interval, mineralization styles correspond mainly to the selective replacement of millimetre to centimetre beds and 0.5 to 3 m thick breccia zones with angular fragments. Mineralization along pre-ore tectonic joints and fractures also account for a minor part of the gold-bearing interval. Tectonic features in this interval include bedding-parallel faults that are notably absent in more thickly bedded successions.

Floatstone beds are interpreted to originate from debris flow events in which sediments are supported above the sediment-water interface by matrix strength and buoyancy, which allows larger clasts to float along in a mud-sand matrix (Moscardelli and Wood, 2008). In this interpretation, sedimentary breccias (floatstone) and clast-bearing mud limestone lithofacies (dark grey to black interval) may coexist over a short distance, reflecting different density flow mechanisms or different ratios of carbonate mud, sand and clasts. Intervals with a granular texture (intraclastic packstone) may also belong to 'mass-transport' deposits, as suggested by the presence of small (mm) angular clasts and may represent the upper and/or distal parts of floatstone intervals (Pinet and Sack, 2019).

Structural control

Fracture density and permeability also influenced mineralizing fluid flow. This general statement is substan-

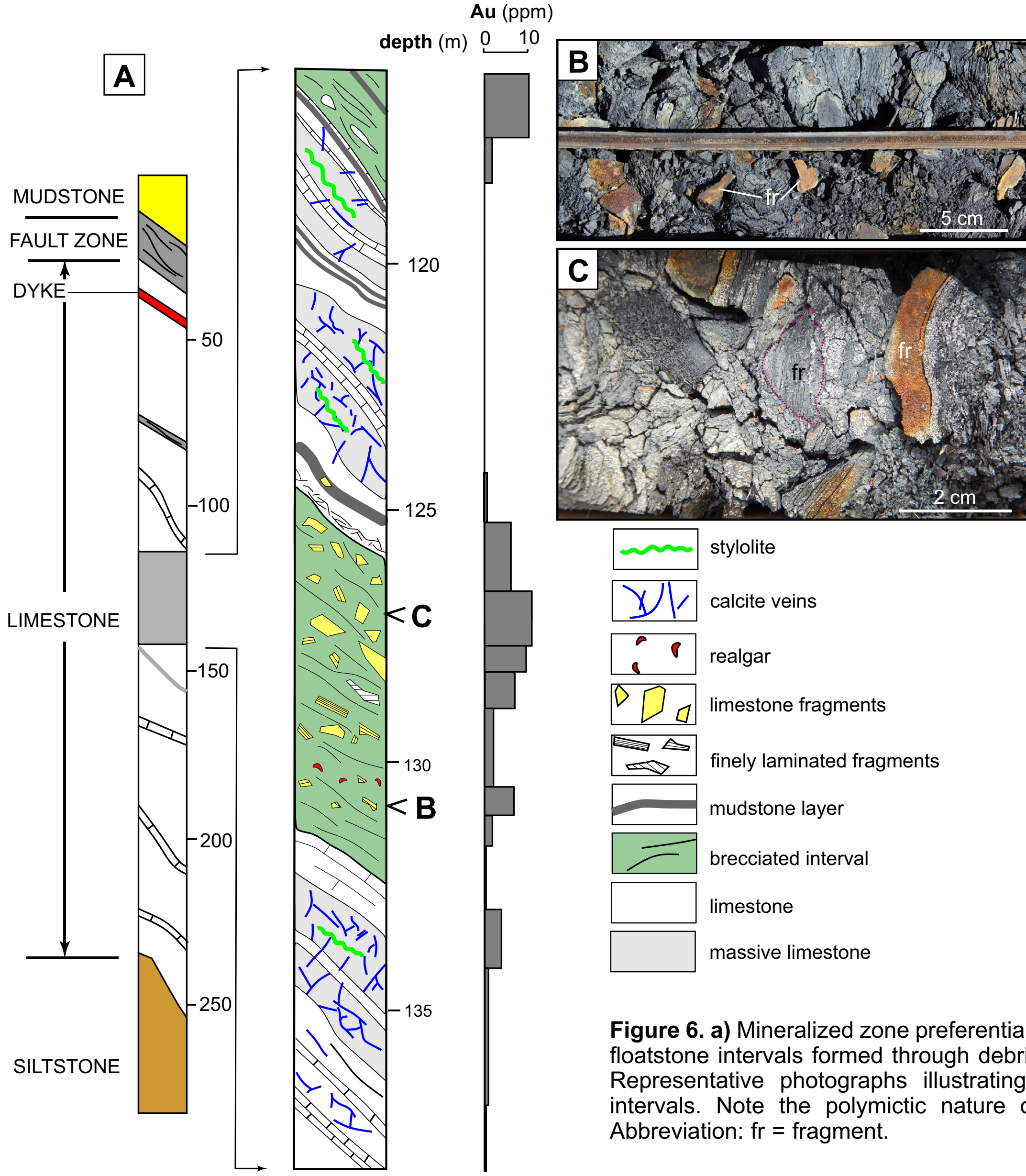

Figure 6. a) Mineralized zone preferentially associated with floatstone intervals formed through debris flows. **b and c)** Representative photographs illustrating the debris flow intervals. Note the polymictic nature of the fragments. Abbreviation: fr = fragment.

tiated by the highest-grade intervals being located in fold hinges with high fracture-density and by the close spatial relationship occurring between fractured rock intervals (i.e. domains with poor rock quality designation, RQD) and gold. Interestingly, intervals above mineralized zones are often characterized by higher than average RQD index values, suggesting that these intervals are less fractured and thus less permeable. Low-permeability domains likely acted as a cap rock for mineralizing fluids. At the tens of metres to hand-sample scales, several types of mineralized structural features can be distinguished.

1. *Mineralized joints.* Among the mineralized structures, some clearly formed as joints under low deviatoric stress, before the main deformation and mineralization events. The joints recorded almost no displacement (tensile-type fractures) and have limited calcite infill. They formed well organized joint sets perpendicular to bedding (Pinet et al., 2020) and contributed to enhance permeability in a way similar to fractured petroleum reservoirs in which there is a clear relationship between the spacing of joints and bed thickness, and in a less pronounced way, between joint spacing and lithology (Rustichelli et al., 2013; Afşar et al., 2014).

2. *Pre-mineralization veins and brecciated intervals.* Pre-mineralization breccias are the most common type of tectonic breccia. At Conrad, the selective replacement of irregular and often complex pre-mineralization vein sets is an important process. Comparison of barren and mineralized samples located a few metres apart (Fig. 8a,b) suggests that calcite between breccia fragments were preferentially dissolved by acidic, early stage mineralizing

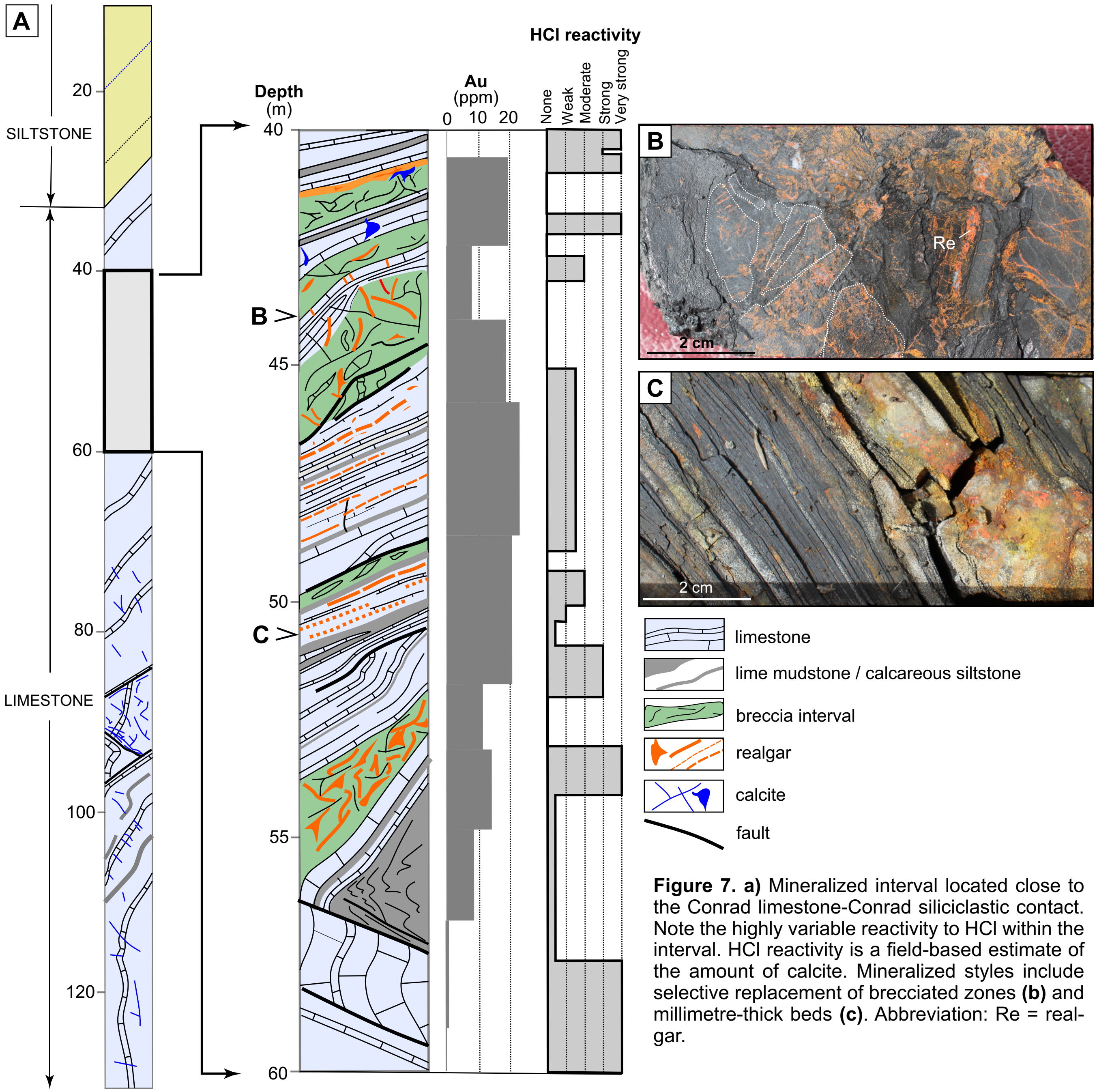

Figure 7. a) Mineralized interval located close to the Conrad limestone-Conrad siliciclastic contact. Note the highly variable reactivity to HCl within the interval. HCl reactivity is a field-based estimate of the amount of calcite. Mineralized styles include selective replacement of brecciated zones **(b)** and millimetre-thick beds **(c)**. Abbreviation: Re = realgar.

fluids, resulting in increased porosity and permeability that focused later gold-bearing fluids. Realgar, orpiment, and fluorite (Fig. 8c) are the most obvious late-mineralization stage minerals in brecciated intervals. Similar to the joints, the amount of pre-mineralization veins and fractures in the pre-mineralization breccia is linked with the structural position (increase in fold hinge zones and fault damaged zones), bed thickness, and lithology (Fig. 8g). Figure 8e and f show an example in which brecciation may be erroneously interpreted as postdating mineralization. In this case, realgar selectively replaces fractures that are mostly confined to the clasts, but closer inspection shows that, in a few cases, realgar-filled veins extend into the matrix, indicating that mineralization postdates fracture and breccia development. Comparison of pre-mineralization breccia intervals within the same drillhole shows a complete transition from barren to realgar-rich gold mineralized rocks (Fig. 8h to j).

3. <u>*Late mineralization stage veins.*</u> Veins associated with the late stage of mineralization are found within and adjacent to (<10 m) gold-bearing intervals. Late mineralization-stage veins are defined by the presence of realgar (±orpiment) and calcite

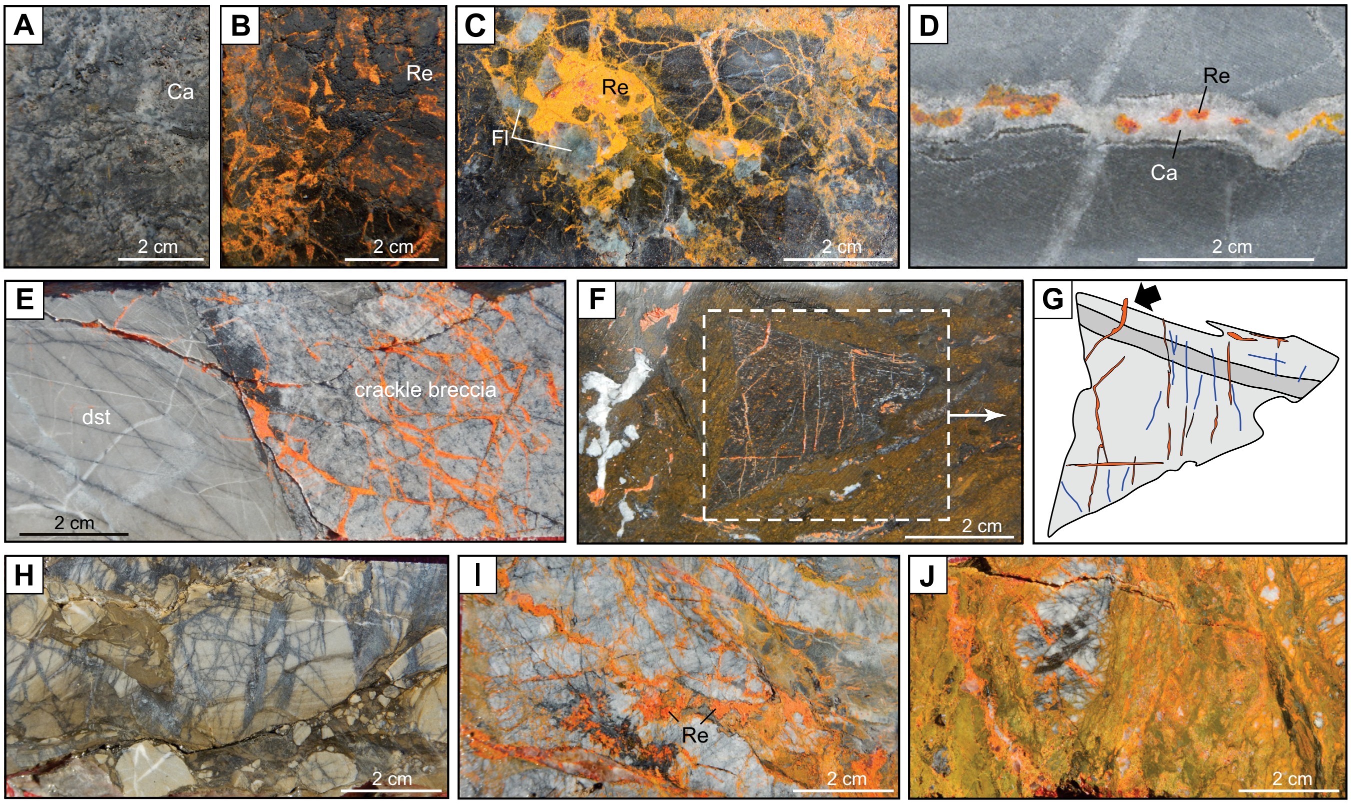

Figure 8. Photographs illustrating the tectonic control on mineralization. Photographs (a) to (f) are from the Conrad zone. Photograph (g) and photographs (h) to (j) are from the Osiris and Sunrise zones, respectively. **a and b)** Comparison of a barren sample (a) and a mineralized sample (b) suggesting that the preferential dissolution of calcite (Ca) between the breccia fragments by early acidic fluids created pathways used by gold-bearing fluids. Abbreviation: Re = realgar **c)** Typical mineralized breccia with fluorite (Fl) and realgar (Re). **d)** Late mineralization calcite (Ca)-realgar (Re) vein crosscutting an earlier calcite vein. **e)** Contact between a massive dolostone bed (dst, left) and a crackle breccia (right). Note that mineralization is almost entirely confined to the crackle breccia. **f and g)** Photograph and interpretation of fractures filled with realgar: most of fractures are confined to a fragment, but one mineralized fracture clearly extends in the matrix (black arrow) indicating that mineralization postdates fragmentation. **h, i, and j)** Photographs of core from within the same drillhole illustrating the transition between barren breccia (h) and realgar (Re)-rich zones in which the pre-existing breccia texture is only locally preserved.

(Fig. 8c). Realgar is found in the central part of the veins or along their margins, suggesting that it both pre- and postdates calcite. The late-stage veins commonly have centimetre-size calcite crystals and, in some cases, a central cavity. In mineralized intervals, these late-stage mineralization veins are visually distinct, but they most likely represent a very small part of the gold endowment. Minor faults cutting calcite-realgar veins attest to some post-veining deformation (Pinet and Sack, 2019).

4. Hydrothermal breccia. In some cases, fracture permeability increased during mineralization and fluid pressure was high enough to fracture rock fragments to form cement-supported breccia ('mosaic breccia'). The amount of cement is variable and locally represents more than 50 vol.% of the rock (Fig. 9d). Cement is typically realgar and/or calcite, but orpiment and, to a lesser extent, fluorite also occur. In the example shown on Figure 9, cement-supported hydrothermal breccia is found below one of the mineralized Conrad mafic dykes. In this case, the local increase in fluid pressure was probably due to the aquitard that was formed by the dyke.

5. Synmineralization fractures and minor faults. Synmineralization brittle faults, with or without cataclasite and gouge development, locally contributed to the development of pathways for mineralizing fluids. Fault planes with realgar slickenlines attest to such syn- to late-mineralization deformation (Pinet and Sack, 2019).

In Conrad, discontinuous gold zones are associated with steeply dipping, northwest-trending fault corridors. For the 350 fault, the zones are located close to the contact between the Conrad limestone and the Conrad siliciclastic rocks, whereas they are entirely hosted in the Conrad siliciclastic rocks in the case of the 850 fault (Fig. 2b, 3). In the latter case, drill core indicates that some deformation occurred during to post mineralization. Tectonic features also include early brittle structures with poorly constrained timing and it is presently unclear if the mineralizing fluids

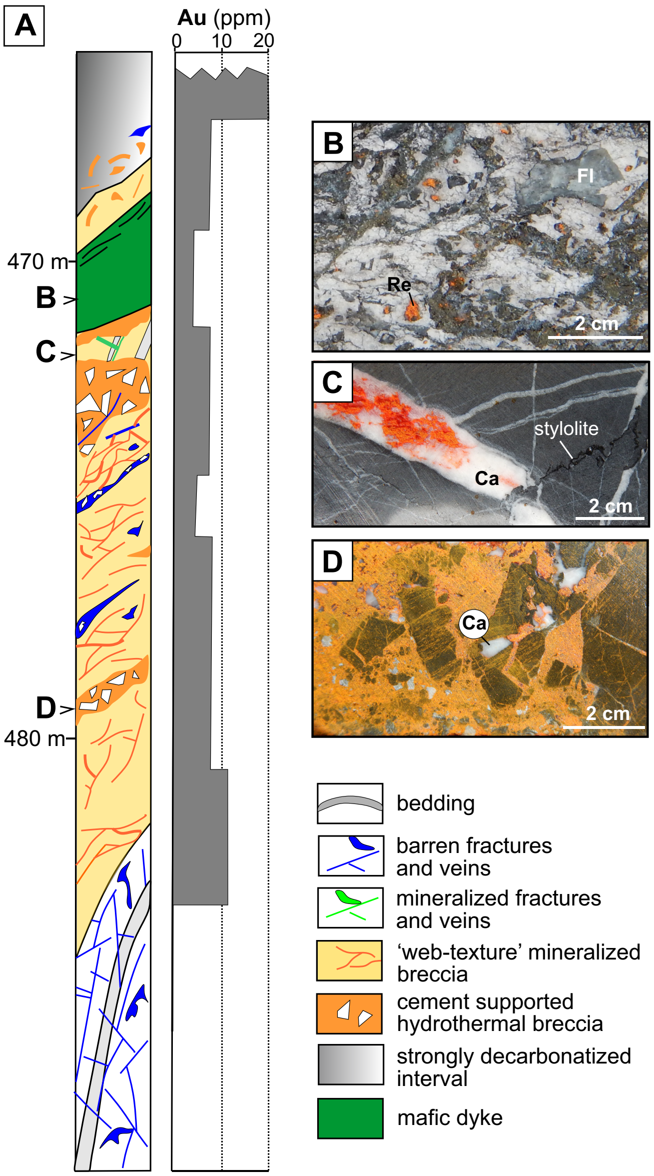

Figure 9. **a)** Mineralized zone with hydrothermal breccia. Note the location of the hydrothermal breccia below a mafic dyke, which probably acted as a local aquitard and contributed to the increase in the fluid pressure. **b)** Mineralized mafic dyke with realgar (Re) and fluorite (Fl). **c)** Late-stage calcite (Ca)-realgar vein. **d)** Hydrothermal breccia in which the chemical matrix represents approximatively 50 vol.% of the rock. Abbreviation: Ca = calcite.

used a pre-existing pathway or if they circulated in an active deformation corridor.

Variations in mineralization styles and feedback effects between sedimentological and tectonic factors

At the macroscopic scale, gold mineralization styles vary significantly, even in the same mineralized interval. Variations in mineralization styles attest to the opportunistic nature of gold-bearing fluids that exploit permeable pathways, regardless of their origin, including floatstone units and intervals characterized by a network of pre-existing fractures. The factors favouring gold mineralization should not be considered separately as sedimentological and tectonic parameters show feedback effects that have resulted in complex mineralized zone geometries. Figure 10 illustrates some of the feedback effects between sedimentological and tectonic controls: 1) due to their high matrix content, floatstone intervals were frequently used as bedding-parallel décollement; 2) fractures acted as feeder pathways for the selective replacement of beds; 3) pre-mineralization fracturing and veining was intimately linked with bed thickness and lithology; and 4) there is a continuum between tectonic and hydrothermal breccia, the only difference being the presumably higher fluid pressure during formation of hydrothermal breccia.

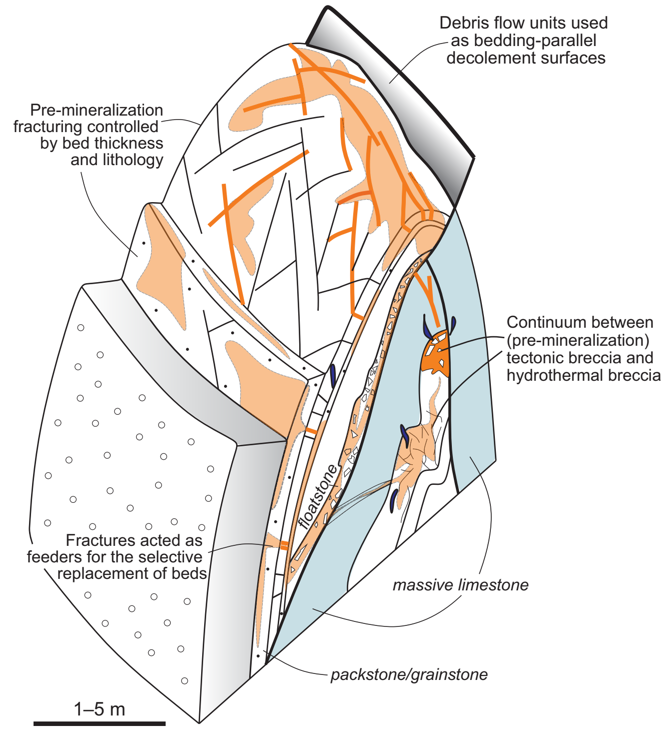

Figure 10. Sketch showing the feedback effects between sedimentological and structural features at the 1 to 5 m scale.

Factors that decrease the permeability also played a major role in focusing mineralizing fluid flow in the Osiris, Sunrise, and Conrad zones. Within the Osiris limestone (Osiris and Sunrise zones), clast-supported rudstone intervals with indented and stylolitic relationships between fragments are never mineralized, even if proximal to gold-bearing intervals (Pinet and Sack, 2019). These discontinuous rudstone intervals acted as impermeable barriers and contributed to the complexity of gold-bearing fluid pathways. A similar interpretation is also valid for thickly (>1 m) bedded limestone intervals at Conrad, which are generally not mineral-

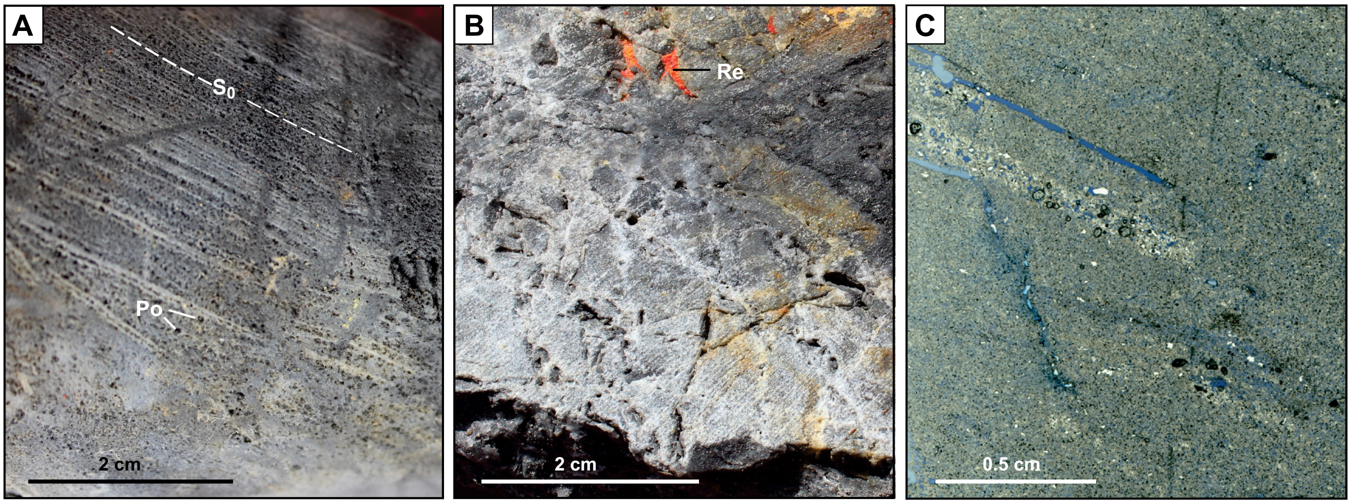

Figure 11. Photographs illustrating the various alteration styles. **a)** Porosity enhancement due to decarbonatization (Sunrise zone). Abbreviations: Po = pore, S_0 = bedding. **b)** Decarbonatization and silicification associated with mineralization (Conrad zone). Abbreviation: Re = realgar. **c)** Thin section showing porosity enhancement due to decarbonatization (Conrad zone). The blue colour corresponds to blue epoxy filling micropores.

ized, even though fractures at high-angle to bedding may have served as by-pass pathways.

Alteration and Gold Mineralization

In the Nadaleen trend, gold deposition resulted from the same processes documented in Nevada (Cline et al., 2005), including an early stage characterized by the dissolution of carbonate, a gold-bearing stage associated with very fine quartz, and a late stage characterized by the deposition of calcite, realgar, orpiment, and fluorite. Alteration associated with gold is restricted to the mineralized zones and immediately surrounding host rocks (generally <1 m).

Within mineralized intervals, decarbonatization (removal of both calcite and dolomite) is the most obvious alteration style. Alteration intensity is highly variable with some decimetre-scale core segments still reacting with HCl a few centimetres from totally decarbonatized core segments (Fig. 7). Decarbonatization is always associated with porosity enhancement. This porosity is sometimes visible at the sample scale (Fig. 11a,b), with some millimetre-wide voids or granular texture and is clear at thin-section scale (Fig. 11c).

Preliminary results of a detailed analysis of Au-bearing arsenian pyrite, here referred to as ore-pyrite, were reported in Sack et al. (2019). Gold-bearing pyrite progressed from early 'blocky' single-stage grains and rims to late 'fuzzy' single-stage grains and rims (Fig. 12). Early, 'blocky' ore-pyrite has low 'Carlin-type' trace element content. Late, 'fuzzy' ore-pyrite has high 'Carlin-type' trace element content. Both types of ore-pyrite are very fine grained. 'Blocky' ore-pyrite has relatively low As and may have precipitated from fluids saturated in Au, with gold partly deposited as nanoparticles. 'Fuzzy' ore-pyrite has higher As content and likely precipitated from an unsaturated fluid with Au incorporated in solid solution. Electron microprobe data suggest that As substitutes for S in both types of ore-pyrite, which is consistent with hydrothermal fluids that were reduced throughout both early and late stages of mineralization. Previous studies have shown that Au and As concentrations decrease in pyrite as temperature of formation increases (Deditius et al., 2014). This retrograde solubility of As (±Au) in ore-pyrite suggests early, 'blocky' pyrite was formed at higher temperatures than late, 'fuzzy' pyrite. Laser-ablation inductively-coupled plasma mass-spectrometry (LA-ICPMS) results show that between 10 and 80% of the gold is contained within very small (<2 µm) single-stage pyrite and the balance is contained in the rims on pre-ore pyrite.

Ore-pyrite is accompanied by variable amounts of silicification through carbonate replacement by fine-grained quartz ('jasperoid'; Lovering, 1972) and very fine quartz lining vugs. Almost all silicified rocks can be scratched, which makes the logging of alteration intensity challenging. No erosion-resistant outcrops of densely silicified rocks (jasperoids) that are locally associated with Carlin-type mineralization in Nevada (Cline et al., 2005) have been found in the Nadaleen trend.

Strong and obvious argillization is rare and reliable estimates of argillization could not be made, even under the microscope, because of their fine grain size and the uncertain genesis of most clay minerals (i.e. hydrothermal or detritic-diagenetic). As mentioned above, realgar, orpiment, and fluorite are ubiquitous in or close to gold-bearing intervals and constitute generally good visual guides for gold mineralization, even if these minerals postdate gold deposition and silicification.

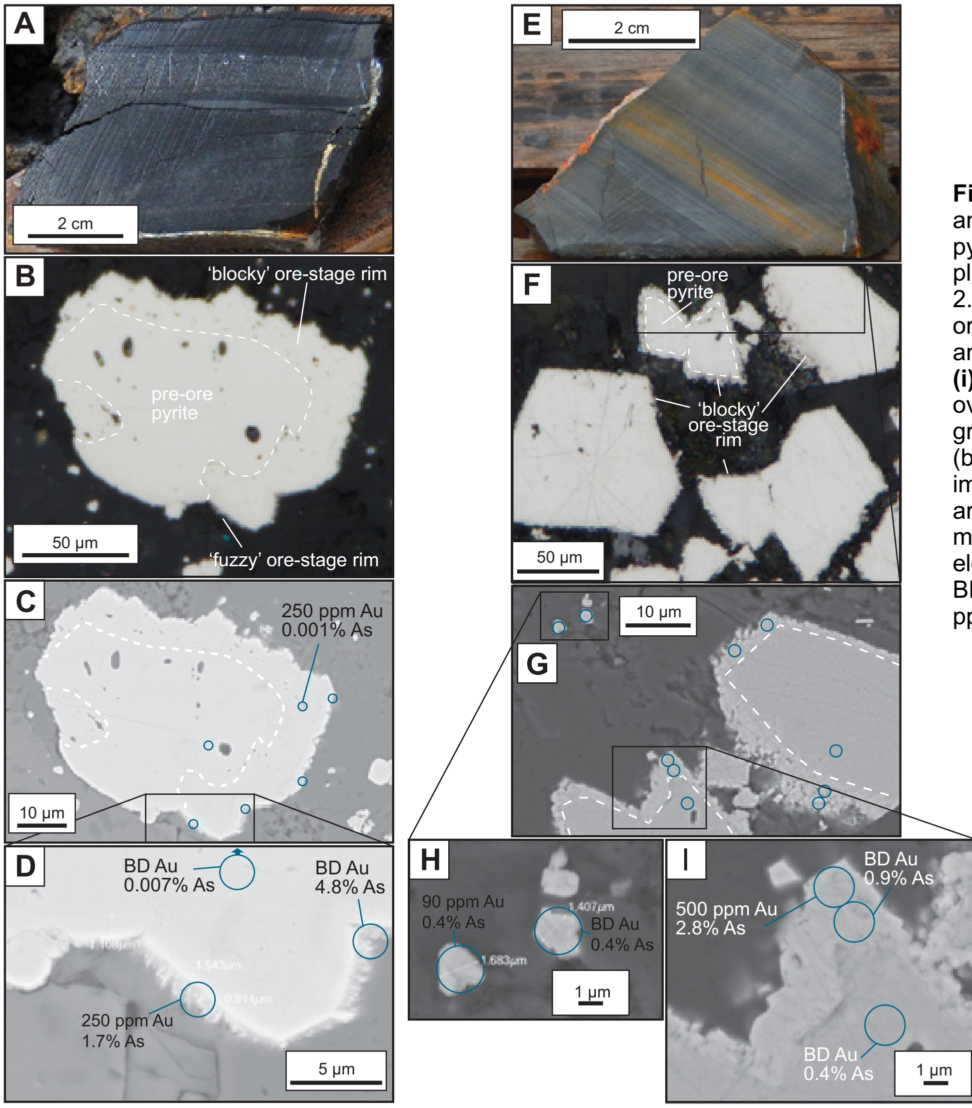

Figure 12. Ore-pyrite from Conrad and Osiris zones. **a to d)** 'Blocky' pyrite with a <1 µm 'fuzzy' rim; sample OS058, 182.8 m (4.5 g/t Au over 2.75 m), Conrad zone. **e to i)** 'Blocky' ore-pyrite as single-stage grains **(h)** and a rim overgrowing pre-ore pyrite **(i)**; sample OS244, 128.0 m (4.9 g/t over 3.04 m), Osiris deposit. Photographs (a) and (e) are of drill core; (b) and (f) are reflected light (50X) images; and (c), (d), (g), (h), and (i) are field emission scanning electron microscope (FE-SEM) backscatter electron (BSE) images. Abbreviation: BD = below detection, which is ~100 ppm Au.

Whole-Rock Geochemistry

The geochemical signature of the gold mineralizing event was investigated using ATAC Resources data. The ATAC Resources database comprises over 29 000 samples assayed for 50 elements, not including Si. The average length of the assayed interval is approximately 3 m. New whole-rock analyses from samples collected along transects from barren rocks to mineralized intervals will be presented in a separate contribution.

Figure 13 presents the correlation coefficients between gold and several elements for the Neoproterozoic-hosted Conrad, Osiris, and Sunrise zones. Thallium, Hg, and As present a high to moderate coefficient of correlation with gold in all three zones. Sulphur and Sb are also positively correlated with gold. Calcium is weakly negatively correlated with gold. However, this weak correlation is mainly due to the original variability of Ca in the host rocks and a clear decrease in Ca content in high-grade (>5 g/t Au) mineralized samples is obvious for the Conrad limestone (Fig. 14; *see* Pinet and Sack, 2019 for a similar plot for the Osiris limestone).

Figure 15 presents the Fe versus S diagram, normalized to Al, the least mobile element (with Ti) among those analyzed. For both the Conrad and Osiris limestone, gold mineralized samples show little or no Fe increase compared to barren samples but a significant enrichment in S. This suggests that S was added to the rock during mineralization but Fe was not, indicating that sulphidation was the dominant process rather than pyritization. Some barren samples have relatively high Fe content, but Fe is probably associated with pre-mineralization ferroan carbonate.

DISCUSSION

Initial Porosity and Permeability Enhancement

In the Nadaleen trend, the preferential occurrence of gold in some sedimentary intervals raises the question of what lithological or alteration features focused fluid flow. In particular, floatstone intervals formed through

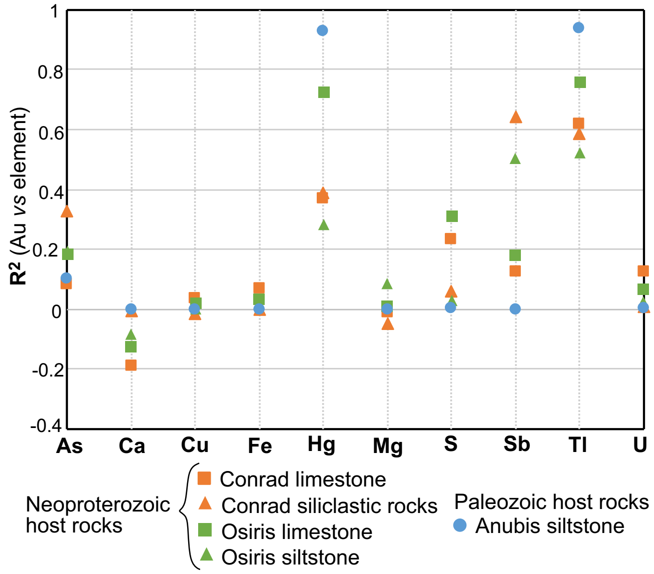

Figure 13. Plot of correlation coefficients between Au and As, Ca, Cu, Fe, Hg, Mg, S, Sb, Tl, and U for several mineralized zones and host rocks. High (>0.5) correlation coefficients are associated with quasi-linear relationships.

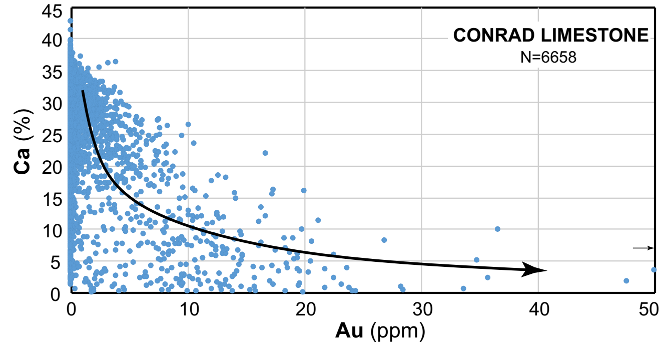

Figure 14. Plot of Au versus Ca for the Conrad limestone showing the decrease in calcium content from decarbonatization as the gold content of samples increases. Samples with low calcium content (Ca <15 wt%) generally indicate intense decarbonatization, however the possibility that the rocks were originally less calcareous than the average rock unit cannot be ruled out.

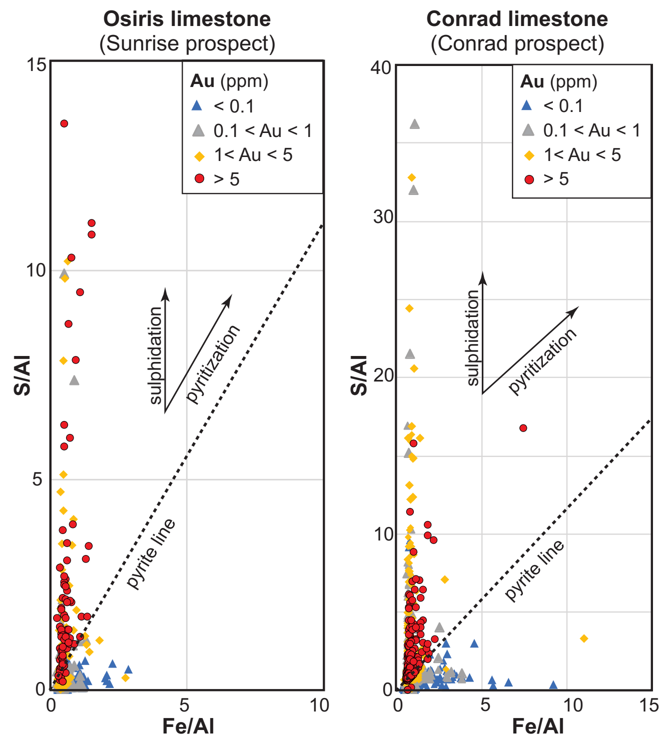

Figure 15. Plots of Fe versus S (normalized with Al) for the Osiris limestone and Conrad limestone. Note that different scales have been used for the two diagrams. In both zones, mineralized samples are characterized by an increase in sulphur.

debris flows are a major host for gold mineralization, suggesting that their original properties contrast with surrounding slope or base-of-slope sedimentary rocks not affected by mass-wasting processes. During debris flow events, clasts 'float' in a mud- to sand-dominated matrix above the sediment-water interface due to matrix strength and buoyancy (Loucks et al., 2010). This results in a slightly higher porosity after mass-wasting compared to the initial, undeformed micrite slope lithofacies. However, the porosity of most carbonate rocks, particularly dominantly mud-rich lithofacies such as those in the Conrad and Osiris limestones, is substantially reduced by early cementation and compaction during burial. Therefore, it seems unlikely that the early (primary) porosity was preserved for >450 Ma between the time of deposition and mineralization. Beaton (2015) proposed that post-depositional dissolution of lime mud and dolomitization of the matrix of the Osiris limestone (Osiris and Sunrise zones) may have contributed to enhance the primary porosity/permeability at the microscale. However, this hypothesis is difficult to consider in the case of the Conrad limestone, which is characterized by sparse and very irregular dolomitization zones at surface and low Mg content (average 0.86 wt%, <2% dolomite if all the Mg is in dolomite). Secondary porosity may also be created through the migration of carbonic acid associated with the generation of carbon dioxide during the maturation of organic matter to hydrocarbon and interaction with subsurface water, but this mechanism remains largely hypothetical in the Nadaleen trend. Whatever the mechanism, hydraulic efficiency of floatstone units was higher than surrounding units during mineralization and was acquired either through the preservation of a secondary porosity or the dissolution of secondary carbonate by early stage acidic hydrothermal fluids.

Pre-mineralization tectonic breccia zones were also probably characterized by a slightly higher fracture permeability than surrounding rocks during the early mineralizing stage. However, in this case, a comparison of barren and mineralized samples suggests that acidic fluids dissolve the calcite infill between fragments more efficiently than the original host rock, enhancing the original porosity and permeability and making these zones effective pathways for late gold-bearing fluids.

Comparison with Paleozoic Rock-Hosted Gold Mineralization

The tight anticline geometry of the Neoproterozoic-hosted gold zones contrasts with the geometry documented for the Paleozoic-hosted zones (including the Anubis area; Fig. 1). The latter are preferentially located along the west-northwest-trending, north-northeast-dipping Anubis fault zone (Moynihan, 2016). The fault zone has a polyphase history with structural events recording predominantly dip-slip and predominantly strike-slip motions (Pinet, unpublished data). Second-order north-northeast-trending faults cut or merge with the Anubis fault.

Mineralization is hosted in a steeply dipping Devonian-Mississippian siliciclastic unit, close to the fault contact with a Middle Devonian dolostone unit. Mineralized intervals are generally highly fractured and are typically difficult to differentiate from the dark grey to black, moderately to non-calcareous, pyrite-rich siltstone and mudstone. In Anubis, the amount of calcite veins, realgar, and orpiment in or close to mineralized intervals is much lower than in Neoproterozoic-hosted zones. Association of gold mineralization with pathfinder elements classically associated with Carlin-type mineralization is also present in Paleozoic-hosted zones, even if some differences with Neoproterozoic zones exist (Fig. 13; absence of correlation with S and Sb, higher correlations with Hg and Tl).

In the absence of temporal constraints on the gold mineralizing event and detailed characterization of mineralizing fluids, Paleozoic gold-bearing zones are tentatively interpreted as a structural end-member (Teal and Jackson, 2002) of Carlin-type mineralization in the Nadaleen trend.

IMPLICATIONS FOR EXPLORATION

Classification of deposit types must be pragmatic and criteria used for defining the specific characteristics of each type should be factual, not interpretative. With this general statement in mind, gold mineralization in the eastern Rackla belt can be classified as a ‘true’ Carlin-type example.

The characteristics consistent with Carlin-type mineralization include the following: 1) host-sedimentary rocks deposited in slope to base-of-slope settings (Moynihan et al., 2019; Pinet et al., 2020); 2) ore-forming events that significantly post-date the ages of the host rocks (Tucker et al., 2018; Davis et al., 2019); 3) the ‘passive’ or ‘opportunistic’ nature of the mineralizing fluids that exploited a variety of porous and permeable pathways regardless of their sedimentary and/or tectonic origin (Pinet and Sack, 2019); 4) alteration that includes partial to complete decalcification of mineralized intervals, and very fine-grained quartz associated with silicification (Tucker et al., 2018); 5) the association of gold with pathfinder elements Tl, As, Hg and Sb, and with minerals such as realgar, orpiment and fluorite (even if the amount of realgar and orpiment is greater than most Carlin-type deposits of Nevada); 6) the low base metal and Ag content of the gold-bearing zones; and 7) the ‘invisible’ nature of gold, which occurs as rims of Au-bearing arsenian pyrite on pre-ore pyrite or as sub-micrometre particles (Sack et al., 2019).

The classification of Nadaleen gold mineralized zones as ‘true’ Carlin-type mineralized zones should not mask the need to refine interpretative models at the upper-crustal to lithospheric scales, which is the aim of ongoing work in the study area.

ONGOING WORK

A better understanding of gold prospects in central Yukon can be achieved only with better geochronological constraints for the age(s) of mineralization. A first step toward this objective was achieved with in situ U-Pb dating on late-stage calcite performed at the Geological Survey of Canada (Ottawa). Preliminary results reported in Davis et al. (2019) show that the U-Pb data from the calcite vein samples exhibit variable degrees of complexity. U-Pb data from three Conrad samples define Tera-Wasserburg intercept ages of between 75 and 72 Ma with relatively simple systematics. Two samples, one from the Osiris zone and one from the Sunrise zone, exhibit complex U-Pb systematics and the dispersion of ages is interpreted to reflect several hydrothermal events, including one at ca. 73 Ma and one or several younger events. The relationship between these hydrothermal pulses and gold mineralization is still under investigation. Ongoing research, including additional U-Pb calcite dating, will provide a tighter control on the age of the gold-mineralizing event and a sound basis to address a number of scientific questions: Is the Carlin-type mineralization event distinct from other metallogenic events documented in the Cordillera? Are other types of mineralization formed contemporaneously? Does the age of mineralization correspond to a change in the magmatic and/or tectonic setting?

Several geochemical methods were used for the characterization of various aspects of the mineralization and results will be reported in future contributions. Geochemical variations due to alteration are investigated through whole rock geochemistry of drillhole samples selected from visually unaltered rocks to altered mineralized zones. The mineralogical content of a few samples was studied through X-ray diffraction to quantitatively study the fine-grained material that may be difficult to characterize with other methods. Hydrothermal fluids and their interaction with host rocks are also being investigated through stable isotope ($\delta^{13}C$ and $\delta^{18}O$) analyses of calcite from several generations of cement and veins, including calcite from late-mineralization veins.

The temperature of mineralizing fluids is being investigated through a fluid inclusion study and clumped isotopes analyses. Fluid inclusion characterization focusses on calcite and fluorite crystals associated with the late-mineralization event. Carbonate clumped-isotopes analysis is a relatively new method with good potential for contributing to hydrothermal fluid characterization (Ghosh et al., 2006). Importantly, thermometry using carbonate clumped-isotopes does not require knowing the isotopic signal of parent water to estimate the precipitation temperature. Analyses were acquired on calcite at the Delta-Lab facility (GSC Quebec) using a Thermo Fisher MAT253 IRMS coupled to a modified KIEL IV carbonate device. To obtain the most precise estimation of the formation temperature of calcite relevant to hydrothermal contexts, the temperature frame was extended to 250°C. This development benefitted from the acquisition of a pressure- and temperature- (T) controlled set-up allowing calcite to be precipitated at high T, linking T to the clumped-isotopic results (Δ_{47} in ‰). An exploratory organic matter study has also been carried out and included Rock-Eval analyses and organic petrography of a few samples to characterize the amount and type of organic matter in dark shale, to investigate the eventual role of organic matter/hydrocarbon in the mineralization processes as well as to qualitatively evaluate the maximum paleo-temperature experienced by the samples.

ACKNOWLEDGMENT

This study is dedicated to Julia Lane who provided tremendous support and scientific inputs. This report beneficiated from discussions with Adam Coulter, and careful analyses were done at the GSC-Quebec, GSC-Calgary, GSC-Ottawa, and University of Nevada laboratories. J. Muntean, C. Lawley, and R. Carne are acknowledged for constructive reviews.

REFERENCES

Afşar, F., Westphal, H., and Philipp, S.L., 2014. How facies and diagenesis affect fracturing of limestone beds and reservoir permeability in limestone-marl alternations; Marine and Petroleum Geology, v. 57, p. 418–432.

Beaton, N.I., 2015. Diagenetic controls on hydrothermal fluid flow in the Osiris, Isis and Isis East Carlin-type showings, Nadaleen Trend, Yukon; M.Sc. thesis, University of Alberta, Edmonton, 180 p.

Cline J.S., Hofstra A., H., Muntean J.L., Tosdal R.M., and Hickey K.A., 2005. Carlin-type gold deposits in Nevada: critical geologic characteristics and viable models; *in* Economic Geology 100th Anniversary volume (1905-2005), (ed.) J.W. Hedenquist, J.F.H. Thompson, R.J. Goldfarb, and J.P Richards; Society of Economic Geologist, p. 541–484.

Davis, W.J., Pinet, N., Petts, D.C., Jackson, S.J., and Mercier-Langevin, P., 2019. U-Pb ages of hydrothermal calcite associated with Carlin-type mineralization, Nadaleen trend, north-central Yukon. Abstract, Geological Association of Canada Annual Meeting. p. 77.

Deditius, A.P., Reich, M., Kesler, S.E., Utsunomiya, S., Chryssoulis, S.L., Walshe, J., and Ewing, R.C., 2014. The coupled geochemistry of Au and As in pyrite from hydrothermal ore deposits; Geochimica et Cosmochimica Acta, v. 140, p. 644–670.

Ghosh, P., Adkins, J., Affek, H., Balta, B., Guo, W., Schauble, E., Schrag, D., and Eiler, J., 2006. ^{13}C-^{18}O bonds in carbonate minerals: A new kind of paleothermometer; Geochimica et Cosmochimica Acta, v. 70, p. 1439–1456

Goodfellow W.D. and Lynch, J.J., 1978. Regional stream sediment and water geochemical reconnaissance data, central Yukon Territory (NTS 106D and parts of 106C, E and F); Geological Survey of Canada, Open File 518, 424 p. (15 sheets).

Loucks, R.G., Kerans, C., Janson, X., and Rajano, M.A.M, 2010. Lithofacies analysis and stratigraphic architecture of a deep-water carbonate debris apron: Lower Cretaceous (Latest Aptian to Latest Albian) Tamabra Formation, Poza Rica field area, Mexico; *in* Mass-Transport Deposits in Deepwater Settings, (ed.) C. Shipp, P. Weimer, and H.W. Posamentier; Society for Sedimentary Geology, Special Publication 95, p. 3367–390.

Lovering, T.G., 1972. Jasperoid in the United States—its characteristics origin and economic significance; U.S. Geological Survey, Professional Paper 710, 164 p.

Moscardelli, L. and Wood, L., 2008. New classification system for mass-transport complexes in offshore Trinidad; Basin Research, v. 20, p. 73–98.

Moynihan D., 2016. Bedrock geology compilation of the eastern Rackla Belt, NTS 105N/15, 105N/16, 105O/13, 106B/4, 106C/1, 106C/2, east-central Yukon; Yukon Geological Survey, Open File 2016-2, 1:75:000 scale.

Moynihan, D., Strauss, J.V., Padget, C.D., and Nelson, L.L., 2019. Upper Windermere Supergroup and the transition from rifting to continent-margin sedimentation, Nadaleen River area, northern Canadian Cordillera; Geological Society of America Bulletin, v. 131, p. 1673–1701.

Muntean, J.L., 2018. The Carlin gold system: Applications to exploration in Nevada and beyond; *in* Diversity of Carlin-Style Gold Deposits, (ed.) J. Muntean; Society of Economic Geologists, Reviews in Economic Geology, v. 20, p. 39–88.

Pinet, N., Sack, P., Mercier-Langevin, P., Lavoie, D., Dubé, B., Lane, J., and Brake, V., 2018. Breccia styles and controls on carbonate replacement-type (‘Carlin-type’) gold zones, Rackla belt, east-central Yukon; *in* Targetted Geoscience Initiative: 2017 Report of Activities, Volume 1, (ed) N. Rogers; Geological Survey of Canada, Open File 8358, p. 136–168.

Pinet, N. and Sack, P., 2019. Macroscopic control on Carlin-type gold mineralization in north-central Yukon; *in* Targeted Geoscience Initiative: 2018 Report of Activities, (ed.) N. Rogers; Geological Survey of Canada, Open File 8549, p. 89–103.

Pinet, N., Sack, P., Mercier-Langevin, P., Colpron, M., Lavoie, D., Dubé, B., and Brake, V.I., 2020. Neoproterozoic-hosted Carlin-type mineralization in central Yukon, part 1: Regional- to prospect-scale geological controls; *in* Targeted Geoscience Initiative 5: Contributions to the Understanding of Canadian Gold Systems, (ed.) P. Mercier-Langevin, C.J.M. Lawley, and S. Castonguay; Geological Survey of Canada, Open File 8712, p. 281–297. doi:10.4095/326045

Ristorcelli, S., Ronning, P., Martin, C., and Christensen, O., 2018. Technical report and estimate of mineral resources for the Osiris project, Yukon, Canada; Technical report submitted to ATAC Resources Ltd.

Rustichelli, A., Agosta, F., Tondi, E., and Spina, V., 2013. Spacing and distribution of bed-perpendicular joints throughout layered, shallow-marine carbonates (Granada Basin, southern Spain); Tectonophysics, v. 582, p. 188–204.

Sack, P., Cline, J., Ren, M., Petts, D., and Pinet, N., 2019. Gold bearing pyrite in Carlin-type gold prospects of the Nadaleen trend, Yukon; Abstract, Geological Association of Canada, Annual Meeting. p. 169.

Teal, L. and Jackson, M., 2002. Geologic overview of the Carlin Trend gold deposits; *in* Gold Deposits of the Carlin Trend, (ed.) T.B. Thompson, L. Teal, and R.O. Meeuwig; Nevada Bureau of Mines and Geology, Bulletin 111, p. 9–19.

Tucker, M.J., Lane, J.C., and Hart, C.J.R., 2018. Overview of Carlin-type prospects of the Nadaleen trend: a Yukon analogue to Carlin-type gold mineralization of the Great Basin; *in* Diversity of Carlin-style gold deposits, (ed.) J.L. Muntean; Society of Economic Geologists, Reviews in Economic Geology, v. 20., p. 235–256.

Appendix 1
Peer-reviewed journal publications related to the TGI-4/TGI-5 gold projects (2015–2020)

Caté, A., Schetselaar, E., Mercier-Langevin, P., and Ross, P.-S., 2018. Classification of lithostratigraphic and alteration units from drillhole lithogeochemical data using machine learning: a case study from the Lalor volcanogenic massive sulphide deposit, Snow Lake, Manitoba, Canada; Journal of Geochemical Exploration, v. 188, p. 216–228. doi:10.1016/j.gexplo.2018.01.019

De Souza, S., Dubé, B., McNicoll, V., Dupuis, C., Mercier-Langevin, P., Creaser, R.A., and Kjarsgaard, I., 2017. Geology and Hydrothermal Alteration of the World-Class Canadian Malartic Gold Deposit: Genesis of an Archean Stockwork-Disseminated Gold Deposit in the Abitibi Greenstoone Belt; *in* Archean Base and Precious Metal Deposits, southern Abitibi Greenstone Belt, Canada, (ed.) T. Monecke, P. Mercier-Langevin, and B. Dubé; Reviews in Economic Geology, v. 19, p. 263–291.

De Souza, S., Dubé, B., Mercier-Langevin, P., McNicoll, V., Dupuis, C., and Kjarsgaard, I., 2019. Hydrothermal alteration mineralogy and geochemistry of the Archean world-class Canadian Malartic disseminated-stockwork gold deposit, southern Abitibi greenstone belt, Quebec, Canada; Economic Geology, v. 114, p. 1057–1094. doi: 10.5382/econgeo.4674

Debreil, J.-A., Ross, P.-S., and Mercier-Langevin, P., 2018. The Matagami district, Abitibi greenstone belt, Canada: Volcanic controls on Archean volcanogenic massive sulfide deposits associated with voluminous felsic volcanism; Economic Geology, v. 113, p. 891–910. doi:10.5382/econgeo.2018.4575

Dubé, B., Mercier-Langevin, P., Ayer, J., Atkinson, B., and Monecke, T., 2017. Orogenic Greenstone-Hosted Quartz-Carbonate Gold Deposits of the Timmins-Porcupine Camp; *in* Archean Base and Precious Metal Deposits, southern Abitibi Greenstone Belt, Canada, (ed.) T. Monecke, P. Mercier-Langevin, and B. Dubé; Reviews in Economic Geology, v. 19, p. 51–79.

Dubosq, R., Lawley, C.J.M., Rogowitz, A., Schneider, D.A., and Jackson, S., 2018. Pyrite deformation and connections to gold mobility: Insight from micro-structural analysis and trace element mapping; Lithos, v. 310-311, p. 86–104. doi:/10.1016/j.lithos.2018.03.024

Dubosq, R., Schneider, D.A., Camacho, A., and Lawley, C.J.M., 2019. Geochemical and geochronological discrimination of biotite types at the Detour Lake Gold Deposit, Canada; Minerals, v. 9., 22 p. doi:10.3390/min9100596

Harmon, R.S., Lawley, C.J.M., Watts, J., Harraden, C.L., Somers, A.M., and Hark, R.R., 2019. Laser-induced breakdown spectroscopy - an emerging analytical tool for mineral exploration; Minerals, v. 9., 45 p. doi:10.3390/min9120718

Lawley, C.J.M., 2016. Compositional symmetry between Earth's crustal building blocks; Geochemical Perspectives Letters, v. 2, p. 117–126. doi:10.7185/geochemlet.1612

Lawley, C.J.M., Creaser, R.A., Jackson, S., Yang, Z., Davis, B., Pehrsson, S., Dubé, B., Mercier-Langevin, P., and Vaillancourt, D., 2015. Unraveling the Western Churchill Province Paleoproterozoic gold metallotect: constraints from Re-Os arsenopyrite and U-Pb xenotime geochronology and LA-ICP-MS arsenopyrite trace element chemistry at the BIF-hosted Meliadine gold district, Nunavut, Canada; Economic Geology, v. 110, p. 1425–1454. doi:10.2113/econgeo.110.6.1425

Lawley, C.J.M., Dubé, B., Mercier-Langevin, P., Kjarsgaard, B., Knight, R., and Vaillancourt, D., 2015. Defining and mapping hydrothermal footprints at the BIF-hosted Meliadine gold district, Nunavut, Canada; Journal of Geochemical Exploration, v. 155, p. 33–55. doi:10.1016/j.gexplo.2015.04.001

Lawley, C.J.M., McNicoll, V., Sandeman, H., Pehrsson, S., Simard, M., Castonguay, S., Mercier-Langevin, P., and Dubé, B., 2016. Age and geological setting of the Rankin Inlet greenstone belt and its relationship to the gold endowment of the Meliadine gold district, Nunavut, Canada; Precambrian Research, v. 275, p. 471–495. doi:10.1016/j.precamres.2016.01.008

Lawley, C.J.M., Jackson, S., Yang, Z., Davis, W., and Eglington, B., 2017. Tracing the transition of gold from source to sponge to sink; Economic Geology, v. 112, p. 169–183. doi:10.2113/econgeo.112.1.169

Lawley, C.J.M., Kjarsgaard, B., Jackson, S.E, Yang, Z., Petts, D. and Roots, E., 2018. Trace metal element and isotopic depth profiles through the Abitibi cratonic mantle; Lithos, v. 314-315, p. 520–533. doi:10.1016/j.lithos.2018.06.026

Lawley, C.J.M., Petts, D.C., Jackson, S.E., Zagorevski, A., Pearson, D.G., Kjarsgaard, B.A., Savard, D., and Tschihart, V., 2019. Precious metal mobility during serpentinization and breakdown of base metal sulphide; Lithos. doi:10.1016/j.lithos.2019.105278

Appendix 1: Peer-reviewed journal publications related to the TGI-4/TGI-5 gold system projects (2015–2020); *in* Targeted Geoscience Initiative 5: Contributions to the Understanding of Canadian Gold Systems, (ed.) P. Mercier-Langevin, C.J.M. Lawley, and S. Castonguay; Geological Survey of Canada, Open File 8712, p. 315–316.

Lawley, C.J.M., Pearson, D.G., Waterton, P., Zagorevski, A., Bédard, J.H., Jackson, S.E., Petts, D.C., Kjarsgaard, B.A., Zhang, S., and Wright, D., 2020. Ore-forming element and isotopic signature of re-fertilized mantle peridotite as determined by nanopowder and olivine LA-ICP-MS analyses; Chemical Geology. doi:10.1016/j.chemgeo.2020.119464

McNicoll, V., Dubé, B., Castonguay, S., Oswald, W., Biczok, J., Mercier-Langevin, P., Skulski, T., and Malo, M., 2016. The world-class Musselwhite BIF-hosted gold deposit, Superior Province, Canada: New high-precision U-Pb geochronology and implications for the geological setting of the deposit and gold exploration; Precambrian Research, v. 272, p. 133–149. doi:10.1016/j.precamres.2015.09.029

Mercier-Langevin, P., Dubé, B., Blanchet, F., Pitre D., and Laberge, A., 2017. The LaRonde Penna Au-rich volcanogenic massive sulfide deposit; *in* Archean Base and Precious Metal Deposits, southern Abitibi greenstone belt, Canada, (ed.) T. Monecke, P. Mercier-Langevin, and B. Dubé; Reviews in Economic Geology, v. 19, p. 225–245.

Mercier-Langevin, P., Simard, M., Dubuc, R., Côté, J., Doucet, P., Daigneault, R., and Gaboury, D., 2017. Geology of the Lapa orogenic gold deposit; *in* Archean Base and Precious Metal Deposits, southern Abitibi Greenstone Belt, Canada, (ed.) T. Monecke, P. Mercier-Langevin, and B. Dubé; Reviews in Economic Geology, v. 19, p. 247–261.

Monecke, P., Mercier-Langevin, P., Dubé, B., and Frieman B.M., 2017. Geology of the Abitibi Greenstone Belt; *in* Archean Base and Precious Metal Deposits, southern Abitibi Greenstone Belt, Canada, (ed.) T. Monecke, P. Mercier-Langevin, and B. Dubé; Reviews in Economic Geology, v. 19, p. 7–49.

Monecke, P., Mercier-Langevin, P., Dubé, B., and Hannington, M., 2017. Archean base and precious metal deposits, southern Abitibi Greenstone Belt, Canada – introduction; *in* Archean Base and Precious Metal Deposits, southern Abitibi Greenstone Belt, Canada, (ed.) T. Monecke, P. Mercier-Langevin, and B. Dubé; Reviews in Economic Geology, v. 19, p. 1–5.

Pilote, J.-L. and Piercey, S.J., 2018. Petrogenesis of the Rambler rhyolite formation: Controls on the Ming VMS deposit and geodynamic implications for the Taconic seaway, Newfoundland Appalachians, Canada; American Journal of Science, v. 318, p. 640–683. doi:10.2475/06.2018.02

Pilote, J.-L., Piercey, S.J., Brueckner, S.M., and Grant, D., 2016. Resolving the relative timing of Au-enrichment in volcanogenic massive sulfide (VMS) deposits using scanning electron microscopy-mineral liberation analyzer: empirical evidence from the Ming deposit, Newfoundland, Canada; Economic Geology, v. 111, p. 1495–1508. doi:10.2113/econgeo.111.6.1495

Pilote, J.-L., Piercey, S., and Mercier-Langevin, P., 2017. Volcanic and structural reconstruction of the deformed and metamorphosed Ming volcanogenic massive sulfide deposit, Canada: implications for ore zone geometry and metal distribution; Economic Geology, v. 112, p. 1305–1332. doi:10.5382/econgeo.2017.4511

Pilote, J.-L., Piercey, S., and Mercier-Langevin, P., 2019. Hydrothermal alteration architecture of the Ming volcanogenic massive sulfide deposit, Baie Verte Peninsula, Newfoundland, Canada; Mineralium Deposita. doi:10.1007/s00126-019-00899-z

Pinet, N., Gloaguen, E., and Giroux, B., 2019. Introduction to this special issue on geophysics applied to mineral exploration: *in* Geophysics Applied to Mineral Exploration, (ed.) N., Pinet, E., Gloaguen, and B., Giroux; Canadian Journal of Earth Sciences, v. 56, p. 5–8. doi:10.1139/cjes-2018-0314

Ross, P.-S., Bourke, A., Mercier-Langevin, P., Lépine, S., Leclerc, F., and Boulerice, A., 2016. High-resolution physical properties, geochemistry and alteration mineralogy for the host rocks of the Archean Lemoine auriferous VMS deposit, Canada; Economic Geology, v. 111, p. 1561–1574. doi:10.2113/econgeo.111.7.1561

Ross, P.-S., Boulerice, A., Mercier-Langevin, P., and McNicoll, V., 2020. Volcanology, chemo-stratigraphy, geochronology, hydrothermal alteration and VMS potential of the Lemoine Member of the Waconichi Formation, Chibougamau district, Abitibi greenstone belt, Québec; Mineralium Deposita, v. 55, p. 21–46. doi:10.1007/s00126-019-00884-6

Schetselaar, E., Bellefleur, G., Craven, J., Roots, E., Cheraghi, S., Shamsipour, P., Caté, A., Mercier-Langevin, P., El Goumi, N., Enkin, R., and Salisbury, M, 2017. Geologically driven 3D modelling of physical rock properties in support of interpreting the seismic response of the Lalor volcanogenic massive sulphide deposit, Snow Lake, Manitoba, Canada; *in* Characterization of Ore-Forming Systems from Geological, Geochemical and Geophysical Studies, (ed.) K., Gessner, T.G., Blenkinsop, P., Sorjonen-Ward; Geological Society, Special Publication 453, p. 57–79. doi:10.1144/SP453.5

Appendix 2
Government publications related to the TGI-4/TGI-5 gold projects (2015–2020)

Beauchamp, A.-M., Dubé, B., Malo, M., McNicoll, V., Archer, P., Lavoie, J., and Chartrand, F., 2015. Geology, mineralization and alteration of the turbidite-hosted Mustang Au showing, Lower Eastmain greenstone belt, Superior Province, Quebec; *in* Targeted Geoscience Initiative 4: Contributions to the Understanding of Precambrian Lode Gold Deposits and Implications for Exploration, (ed.) B. Dubé and P. Mercier-Langevin; Geological Survey of Canada, Open File 7852, p. 227–243. doi:10.4095/296624

Bleeker, W., 2015. Syn-orogenic gold mineralization in granite-greenstone terranes: the deep connection between extension, major faults, syn-orogenic clastic basins, magmatism, thrust inversion and long-term preservation; *in* Targeted Geoscience Initiative 4: Contributions to the Understanding of Precambrian Lode Gold Deposits and Implications for Exploration, (ed.) B. Dubé and P. Mercier-Langevin; Geological Survey of Canada, Open File 7852, p. 25–47. doi:10.4095/296624

Boily-Auclair, É., Mercier-Langevin, P., Ross, P.-S., and Pitre, D., 2019. Lithological and structural controls on the nature and distribution of gold at the LaRonde Zone 5 project, Doyon-Bousquet-LaRonde gold camp, Abitibi, Quebec; *in* Targeted Geoscience Initiative: 2018 report of activities, (ed.) N. Rogers; Geological Survey of Canada, Open File 8549, p. 23–32. doi: 10.4095/313631

Boily-Auclair, É., Mercier-Langevin, P., Ross, P.-S., and Pitre, D., 2020. Stratigraphic setting of the LZ5 and Ellison mineralized zones, LaRonde Zone 5 project, Doyon-Bousquet-LaRonde mining camp, Abitibi, Quebec; *in* Targeted Geoscience Initiative 5: Contributions to the Understanding of Canadian Gold Systems, (ed.) P. Mercier-Langevin, C.J.M. Lawley, and S. Castonguay; Geological Survey of Canada, Open File 8712, p. 57–73. doi.org/10.4095/323665

Boudreau, C., Mercier-Langevin, P., Krushnisky, A., and Goutier, J., 2020. Sulphide clast-bearing felsic volcaniclastic units of the Rouyn-Pelletier Formation: Comparison with similar units of the Horne Block, Rouyn-Noranda, Abitibi greenstone belt, Quebec; *in* Targeted Geoscience Initiative 5: Contributions to the Understanding of Canadian Gold Systems, (ed.) P. Mercier-Langevin, C.J.M. Lawley, and S. Castonguay; Geological Survey of Canada, Open File 8712, p. 45–56. doi:10.4095/323664

Boulerice, A.R., Ross, P.-S., and Mercier-Langevin, P., 2015. Geological and geochemical characteristics of the Waconichi Formation east of the Lemoine auriferous volcanogenic massive sulphide deposit, Abitibi greenstone belt, Quebec; *in* Targeted Geoscience Initiative 4: Contributions to the Understanding of Volcanogenic Massive Sulphide Deposit Genesis and Exploration Methods Development, (ed.) J.M. Peter and P. Mercier-Langevin; Geological Survey of Canada, Open File 7853, p. 171–182. doi:10.4095/296540

Castonguay, S., Ootes, L., Mercier-Langevin, P., Rowins, S., and Devine, F., 2017. Orogenic gold along Cordilleran faults: Key characteristics and analogies between Phanerozoic and Archean settings; *in* Targeted Geoscience Initiative: 2016 report of activities, (ed.) N. Rogers; Geological Survey of Canada, Open File 8199, p. 35–37. doi:10.4095/299585

Castonguay, S., Dubé, B., Mercier-Langevin, P., McNicoll, V.J., DeLazeer, A., and Malcolm, K., 2018. Nature and significance of deformation zones on gold mineralization in the Detour Lake area: Implications for exploration in Ontario and Quebec; *in* Targeted Geoscience Initiative: 2017 report of activities, volume 1, (ed.) N. Rogers; Geological Survey of Canada, Open File 8358, p. 105–111. doi:10.4095/306441

Castonguay, S., Ootes, L., Mercier-Langevin, P., and Devine, F., 2018. Gold along Cordilleran faults: Key characteristics and analogies between Phanerozoic and Archean settings; *in* Targeted Geoscience Initiative: 2017 report of activities, volume 1, (ed.) N. Rogers; Geological Survey of Canada, Open File 8358, p. 139–145. doi: 10.4095/306460

Castonguay, S., Dubé, B., Mercier-Langevin, P., and Wodicka, N., 2019. Geological setting and mineralization styles of the Sunday Lake and Lower Detour 'gold trends', northwestern Abitibi greenstone belt, Ontario and Quebec; *in* Targeted Geoscience Initiative: 2018 report of activities, (ed.) N. Rogers; Geological Survey of Canada, Open File 8549, p. 9–22. doi:10.4095/313625

Castonguay, S., Dubé, B., Wodicka, N., and Mercier-Langevin, P., 2020. Geological setting and gold mineralization associated with the Sunday Lake and Lower Detour deformation zones, northwestern Abitibi greenstone belt, Ontario and Quebec; *in* Targeted Geoscience Initiative 5: Contributions to the Understanding of Canadian Gold Systems, (ed.) P. Mercier-Langevin,

Appendix 2: Government publications related to the TGI-4/TGI-5 gold system projects (2015–2020); *in* Targeted Geoscience Initiative 5: Contributions to the Understanding of Canadian Gold Systems, (ed.) P. Mercier-Langevin, C.J.M. Lawley, and S. Castonguay; Geological Survey of Canada, Open File 8712, p. 317–325.

C.J.M. Lawley, and S. Castonguay; Geological Survey of Canada, Open File 8712, p. 127–142. doi:10.4095/323670

Castonguay, S., Ootes, L., Devine, F., and Friedman., R., 2020. Superimposed Late Cretaceous and earliest Eocene gold mineralization and deformation events along the Llewellyn-Tally Ho deformation corridor in northwest British Columbia and southern Yukon; *in* Targeted Geoscience Initiative 5: Contributions to the Understanding of Canadian Gold Systems, (ed.) P. Mercier-Langevin, C.J.M. Lawley, and S. Castonguay; Geological Survey of Canada, Open File 8712, p. 223–236. doi:10.4095/326039

Caté, A., Mercier-Langevin, P., Ross, P.-S., Duff, S., Hannington, M.D., Dubé, B., and Gagné, S., 2015. Geology and Au enrichment processes at the Paleoproterozoic Lalor auriferous volcanogenic massive sulphide deposit, Snow Lake, Manitoba; *in* Targeted Geoscience Initiative 4: Contributions to the Understanding of Volcanogenic Massive Sulphide Deposit Genesis and Exploration Methods Development, (ed.) J.M. Peter and P. Mercier-Langevin; Geological Survey of Canada, Open File 7853, p. 131–145. doi:10.4095/296540

Caté, A., Mercier-Langevin, P., Ross, P.-S., Bécu, V., Lauzière, K., Hannington, M., Duff. S., Dubé, B., and Gagné, S., 2017. Whole-rock lithogeochemistry of the Lalor auriferous volcanogenic massive-sulfide deposit, Manitoba; Geological Survey of Canada, Open File 8107, 1 .zip file.

Ciufo, T.J., Yakymchuk, C., Lin, S., Jellicoe, K., and Mercier-Langevin, P., 2018. Hydrothermal alteration and vectors at the orogenic Island Gold deposit, Michipicoten greenstone belt, Wawa, Ontario; *in* Targeted Geoscience Initiative: 2017 report of activities, volume 1, (ed.) N. Rogers; Geological Survey of Canada, Open File 8358, p. 117–120. doi:10.4095/306443

Ciufo, T.J., Mercier-Langevin, P., Yakymchuk, C., Lin, S., Bécu, V., and Lauzière, K., 2019. Whole-rock lithogeochemistry of the Archean Islang Gold deposit, Ontario, Canada; Geological Survey of Canada, Open File 8524, 1 .zip file. doi:10.4095/314791

Ciufo, T.J., Jellicoe, K., Yakymchuk, C., Lin, S., Mercier-Langevin, P., and Wodicka, N., 2020. Geology, structural evolution, and hydrothermal alteration of the Island Gold deposit, Michipicoten greenstone belt, Ontario; *in* Targeted Geoscience Initiative 5: Contributions to the Understanding of Canadian Gold Systems, (ed.) P. Mercier-Langevin, C.J.M. Lawley, and S. Castonguay; Geological Survey of Canada, Open File 8712, p. 143–156. doi:10.4095/323671

Davis, W.J., McNicoll, V.J., Mercier-Langevin, P., Dubé, B., Rhys, D., Jackson, S.E., Lawley, C.J.M., and Hunt, P.A, 2017. New approaches to dating hydrothermal gold deposits; *in* Targeted Geoscience Initiative: 2016 report of activities, (ed.) N. Rogers; Geological Survey of Canada, Open File 8199, p. 27–28. doi:10.4095/299582

De Souza, S., Dubé, B., McNicoll, V., Dupuis, C., Mercier-Langevin, P., Creaser, R.A., and Kjarsgaard, I., 2015. Geology, hydrothermal alteration, and genesis of the world-class Canadian Malartic stockwork-disseminated Archean gold deposit, Abitibi, Quebec; *in* Targeted Geoscience Initiative 4: Contributions to the Understanding of Precambrian Lode Gold Deposits and Implications for Exploration, (ed.) B. Dubé and P. Mercier-Langevin; Geological Survey of Canada, Open File 7852, p. 113–126. doi:10.4095/296624

De Souza, S., Dubé, B., McNicol, V., Mercier-Langevin, P., Creaser, R.A., and Kjarsgaard, I., 2017. (Day 5 – Part I) Geology and disseminated-stockwork gold mineralization at the world-class Canadian Malartic mine, Abitibi greenstone belt, Canada; Chapter 8 *in* Precious- and Base-Metal Deposits of the southern Abitibi Greenstone Belt, Superior Province, Canada: A field trip to the 14th Biennial Society for Geology Applied to Mineral Deposits meeting, (ed.) P. Mercier-Langevin, J. Goutier, and B. Dubé; Geological Survey of Canada, Open File 8317, p. 55–64. doi:10.4095/306259

Dubé, B., Mercier-Langevin, P., Castonguay, S., McNicoll, V.J., Bleeker, W., Lawley, C.J.M., De Souza, S., Jackson, S.E., Dupuis, C., Gao, J.-F., Bécu, V., Pilote, P., Goutier, J., Beakhouse, G.P., Yergeau, D., Oswald, W., Janvier, V., Fontaine, A., Pelletier, M., Beauchamp, A.-M., Katz, L.R., Kontak, D.J., Tóth, Z., Lafrance, B., Gourcerol, B., Thurston, P.C., Creaser, R.A., Enkin, R.J., El Goumi, N., Grunsky, E.C., Schneider, D.A., Kelly, C.J., and Lauzière, K., 2015. Precambrian lode gold deposits — a summary of TGI-4 contributions to the understanding of lode gold deposits, with an emphasis on implications for exploration; *in* Targeted Geoscience Initiative 4: Contributions to the Understanding of Precambrian Lode Gold Deposits and Implications for Exploration, (ed.) B. Dubé and P. Mercier-Langevin; Geological Survey of Canada, Open File 7852, p. 1–24. doi:10.4095/296624.

Duff, S., Hannington, M., Caté, A., Mercier-Langevin, and Kjarsgaard, I.J., 2015. Major ore types of the Paleoproterozoic Lalor auriferous volcanogenic massive sulphide deposit, Snow Lake, Manitoba; in Targeted Geoscience Initiative 4: Contributions to the Understanding of Volcanogenic Massive Sulphide Deposit Genesis and Exploration Methods Development, (ed.) J.M. Peter and P. Mercier-Langevin; Geological Survey of Canada, Open File 7853, p. 147–170. doi:10.4095/296540

El Goumi, N., De Souza, S., Enkin, R.J., and Dubé, B., 2015. Petrophysical signature of gold mineralization and alteration assemblages at the Canadian Malartic deposit, Quebec, Canada; *in* Targeted Geoscience Initiative 4: Contributions to the Understanding of Precambrian Lode Gold Deposits and Implications for Exploration, (ed.) B. Dubé and P. Mercier-Langevin; Geological Survey of Canada, Open File 7852, p. 127–138. doi:10.4095/296624

Fayard, Q., Mercier-Langevin, P., Daigneault, R., and Perreault, S., 2018. Volcanic, hydrothermal and structural controls on the nature and distribution of base and precious metals at the B26 project, Brouillan volcanic complex, Abitibi, Quebec; *in* Targeted Geoscience Initiative: 2017 report of activities, volume 1, (ed.) N. Rogers; Geological Survey of Canada, Open File 8358, p. 99–103. doi:10.4095/306440

Fayard, Q., Mercier-Langevin, P., Wodicka, N., Daigneault, R., and Perreault, S., 2020. The B26 Cu-Zn-Ag-Au project, Brouillan volcanic complex, Abitibi greenstone belt, part 1: Geological setting and geochronology; *in* Targeted Geoscience Initiative 5: Contributions to the Understanding of Canadian Gold Systems, (ed.) P. Mercier-Langevin, C.J.M. Lawley, and S. Castonguay; Geological Survey of Canada, Open File 8712, p. 93–107. doi:10.4095/323668

Fayard, Q., Mercier-Langevin, P., Daigneault, R., Perreault, S., and Wodicka, N., 2020. The B26 Cu-Zn-Ag-Au project, Brouillan volcanic complex, Abitibi greenstone belt, part 2: Hydrothermal alteration and mineralization; *in* Targeted Geoscience Initiative 5: Contributions to the Understanding of Canadian Gold Systems, (ed.) P. Mercier-Langevin, C.J.M. Lawley, and S. Castonguay; Geological Survey of Canada, Open File 8712, p. 109–125. doi:10.4095/323669

Fontaine, A., Dubé, B., Malo, M., McNicoll, V., Brisson, T., and Doucet, D., 2015. Geology of the metamorphosed Roberto gold deposit (Éléonore Mine), Baie-James region, Québec: Diversity of mineralization styles in a polyphase tectono-metamorphic setting; *in* Targeted Geoscience Initiative 4: Contributions to the Understanding of Precambrian Lode Gold Deposits and Implications for Exploration, (ed.) B. Dubé and P. Mercier-Langevin; Geological Survey of Canada, Open file 7852, p. 209–225. doi:10.4095/296624

Fontaine, A., Dubé, B., Malo, M., McNicoll, V.J., Prud'homme, N., Beausoleil, C., and Goutier, J., 2018. Geology of the Éléonore gold mine and adjacent gold showings, Superior Province, northern Quebec; *in* Targeted Geoscience Initiative: 2017 report of activities, volume 1, (ed.) N. Rogers; Geological Survey of Canada, Open File 8358, p. 121–125. doi:10.4095/306444

Gao, J.-F., Jackson, S.E., Dubé, B., and De Souza, S., 2015. Genesis of the Canadian Malartic, Côté Gold, and Musselwhite gold deposits: Insights from LA-ICP-MS element mapping of pyrite; *in* Targeted Geoscience Initiative 4: Contributions to the Understanding of Precambrian Lode Gold Deposits and Implications for Exploration, (ed.) B. Dubé and P. Mercier-Langevin; Geological Survey of Canada, Open file 7852, p. 157–175. doi:10.4095/296624

Gill, S.B., Piercey, S.J., Layton-Matthews, D., Layne, G.D., and Piercey, G., 2015. Mineralogical, sulphur, and lead isotopic study of the Lemarchant Zn-Pb-Cu-Ag-Au-VMS deposit: Implications for precious-metal enrichment processes in the VMS environment; *in* Targeted Geoscience Initiative 4: Contributions to the Understanding of Volcanogenic Massive Sulphide Deposit Genesis and Exploration Methods Development, (ed.) J.M. Peter and P. Mercier-Langevin; Geological Survey of Canada, Open File 7853, p. 183–195. doi:10.4095/296540

Gosselin, P. and Dubé, B., 2015. World lode gold deposit database; Geological Survey of Canada, Open File 7930, 27 p. doi:10.4095/297322

Gourcerol, B., Thurston, P.C., Kontak, D.J., Côté-Mantha, O., and Biczok, J., 2015. Depositional setting of Algoma-type banded iron formation from the Meadowbank, Meliadine, and Musselwhite gold deposits; *in* Targeted Geoscience Initiative 4: Contributions to the Understanding of Precambrian Lode Gold Deposits and Implications for Exploration, (ed.) B. Dubé and P. Mercier-Langevin; Geological Survey of Canada, Open File 7852, p. 55–68. doi:10.4095/296624

Gourcerol, B., Thurston, P.C., Kontak, D.J., Côté-Mantha, O., and Biczok, J., 2015. Distinguishing primary and mineralization-related signatures of chert from the banded iron formation-type gold deposits at Musselwhite, Ontario and Meadowbank, Nunavut; Geological Survey of Canada, Current Research 2015-1, 21 p. doi:10.1095/295531

Grondin-LeBlanc, P., Mercier-Langevin, P., Malo, M., Côté-Mantha, O., Simard, M., Barbe, P., Valette, M., and De Souza, S., 2017. Structural controls on the nature and distribution of gold in polytectonized Precambrian volcano-sedimentary successions: An example from the Whale Tail Zone, Amaruq project, Nunavut; Geological Survey of Canada, Scientific Presentation 63, 1 sheet. doi:10.4095/300660

Grunsky, E.C., Brauhart, C.W., Hagemann, S., and Dubé, B., 2015. The magmato-hydrothermal space: a new metric for geochemical characterization of ore deposits; Geological Survey of Canada, Open File 7487, 1 sheet. doi:10.4095/295662

Grunsky, E.C., Dubé, B., Hagemann, S., and Brauhart, C., 2015. A Global Database of Gold Deposits: Quantification of Multi-element Ore Signatures; in Targeted Geoscience Initiative 4: Contributions to the Understanding of Precambrian Lode Gold Deposits and Implications for Exploration, (ed.) B. Dubé and P. Mercier-Langevin; Geological Survey of Canada, Open file 7852, p. 271–285. doi:10.4095/296624

Honsberger, I. and Bleeker, W., 2018. Orogenic comparison of structurally controlled gold systems of the Abitibi Greenstone Belt and central Newfoundland Appalachians: implications for Newfoundland gold potential and recurring tectonic drivers of gold mineralization; *in* Targeted Geoscience Initiative: 2017 report of activities, volume 2, (ed.) N. Rogers; Geological Survey of Canada, Open File 8373, p. 65–70. doi: 10.4095/306602

Honsberger, I.W., Bleeker, W., Kamo, S.L., Evans, D.T.W., and Sandeman, H.A.I., 2019. A Neoproterozoic age for granodiorite underlying Rogerson Lake Conglomerate:

Confirmed Ganderian basement in the Wilding Lake area, central Newfoundland gold district; Government of Newfoundland and Labrador, Department of Natural Resources, Geological Survey, Open File 012A/07/1774, 12 p.

Honsberger, I.W., Bleeker, W., Sandeman, H.A.I., and Evans, D.T.W., 2019. Lithological and structural setting of structurally controlled gold mineralization in the Wilding Lake region, central Newfoundland; *in* Targeted Geoscience Initiative: 2018 report of activities, (ed.) N. Rogers; Geological Survey of Canada, Open File 8549, p. 59–69. doi:10.4095/313640

Honsberger, I.W., Bleeker, W., Sandeman, H.A.I., and Evans, D.T.W., 2019. Structural geology of a gold-bearing quartz vein system, Wilding Lake region, central Newfoundland; *in* Current Research; Geological Survey of Newfoundland and Labrador, Department of Natural Resources,Geological Survey, Report 19-1, p. 23–28.

Honsberger, I.W., Bleeker, W., Sandeman, H.A.I., Evans, D.T.W., and Kamo, S.L., 2019. Structurally controlled gold system, Antler Gold Inc.'s Wilding Lake property, central Newfoundland; Government of Newfoundland and Labrador, Department of Natural Resources, Geological Survey, Open File 012A/1811, 12 p.

Honsberger, I.W., Bleeker, W., Kamo, S.L., Sandeman, H.A.I., and Evans, D.T.W., 2020. The emerging Paleozoic gold district of central Newfoundland: New insights on structural controls and tectonic drivers of gold mineralization and preservation; *in* Targeted Geoscience Initiative 5: Contributions to the Understanding of Canadian Gold Systems, (ed.) P. Mercier-Langevin, C.J.M. Lawley, and S. Castonguay; Geological Survey of Canada, Open File 8712, p. 193–210. doi:10.4095/326024

Honsberger, I.W., Bleeker, W., Sandeman, H.A.I., Evans, D.T.W., and Kamo, S.L., 2020. Vein-hosted gold mineralization in the Wilding Lake area, central Newfoundland: Structural geology and vein evolution; *in* Targeted Geoscience Initiative 5: Contributions to the Understanding of Canadian Gold Systems, (ed.) P. Mercier-Langevin, C.J.M. Lawley, and S. Castonguay; Geological Survey of Canada, Open File 8712, p. 179–191. doi:10.4095/326020

Honsberger, I.W., Bleeker, W., Sandeman, H.A.I., Evans, D.T.W., and Kamo, S.L., 2020. The Wilding Lake gold prospect in central Newfoundland: A lithological and structural synthesis; Geological Survey of Canada, Open File 8658, 2 sheet. doi:10.4095/321490

Janvier, V., Castonguay, S., Mercier-Langevin, P., Dubé, B., Malo, M., McNicoll, V., Creaser, R.A., de Chavigny, B., and Pehrsson, S., 2015. Geology of the banded iron formation-hosted Meadowbank gold deposit, Churchill Province, Nunavut; *in* Targeted Geoscience Initiative 4: Contributions to the Understanding of Precambrian Lode Gold Deposits and Implications for Exploration, (ed.) B. Dubé and P. Mercier-Langevin; Geological Survey of Canada, Open File 7852, p. 255–269. doi:10.4095/296624

Janvier, V., Castonguay, S., Mercier-Langevin, P., Dubé, B., McNicoll, V., Pehrsson, S., Malo, M., De Chavigny, B., and Côté-Mantha, O., 2015. Preliminary results of the geology of the Portage deposit, Meadowbank gold mine, Churchill Province, Nunavut; Geological Survey of Canada, Current Research 2015-2, 21 p. doi:10.4095/295532

Jellicoe, K.M., Lin, S., Ciufo, T.J., Yakymchuk, C., and Mercier-Langevin, P., 2018. Structural controls and relative timing of events at the orogenic Island Gold deposit, Michipicoten greenstone belt, Wawa, Ontario; *in* Targeted Geoscience Initiative: 2017 report of activities, volume 1, (ed.) N. Rogers; Geological Survey of Canada, Open File 8358, p. 113–116. doi:10.4095/306442

Katz, L.R., Kontak, D.J., Dubé, B., and McNicoll, V., 2015. The Archean Côté gold intrusion-related Au (-Cu) deposit, Ontario, Canada: A large-tonnage, low-grade deposit centred on a magmatic-hydrothermal breccia; *in* Targeted Geoscience Initiative 4: Contributions to the Understanding of Precambrian Lode Gold Deposits and Implications for Exploration, (ed.) B. Dubé and P. Mercier-Langevin; Geological Survey of Canada, Open File 7852, p. 139–155. doi:10.4095/296624

Katz, L.R., Kontak, D.J., Dubé, B., Mercier-Langevin, P., Bécu, V., and Lauzière, K., 2016. Whole-rock lithogeochemistry of the Archean intrusion-related Côté Gold Au(-Cu) deposit, Ontario, Canada; Geological Survey of Canada, Open File 8040, 5 p., 1 .zip file. doi:10.4095/299354

Kelly, C.J. and Schneider, D.A., 2015. Insights into the timing of mineralization and metamorphism in the North Caribou Greenstone Belt, Western Superior Province; *in* Targeted Geoscience Initiative 4: Contributions to the Understanding of Precambrian Lode Gold Deposits and Implications for Exploration, (ed.) B. Dubé and P. Mercier-Langevin; Geological Survey of Canada, Open File 7852, p. 245–253. doi:10.4095/296624

Krushnisky, A., Mercier-Langevin, P., Ross, P.-S., Bécu, V., Lauzière, K., and Goutier, J., 2017. Whole-rock lithogeochemistry of the gold-bearing mineralized zones of the Horne 5 deposit, Québec, Canada; Geological Survey of Canada, Open File 8501, 1 .zip file. doi: 10.4095/314545

Krushnisky, A., Mercier-Langevin, P., Ross, P.-S., Goutier, J., Pilote, C., Bernier, C., and Moore, L., 2017. (Day 3 – Part II) The Horne 5 deposit; Chapter 6 *in* Precious- and Base-Metal Deposits of the southern Abitibi Greenstone Belt, Superior Province, Canada: A field trip to the 14th Biennial Society for Geology Applied to Mineral Deposits meeting, (ed.) P. Mercier-Langevin, J. Goutier, and B. Dubé; Geological Survey of Canada, Open File 8317, p. 41–47. doi:10.4095/306257

Krushnisky, A., Mercier-Langevin, P., Ross, P.-S., McNicoll, V., Goutier, J., Moore, L., Pilote, C., and Bernier, C., 2017. The Au-Ag-Cu-Zn-bearing mineralized zones at the Horne 5 deposit, Rouyn-Noranda, Quebec – New observations and preliminary results; Geological Survey of Canada, Scientific Presentation 62, 1 sheet. doi: 10.4095/300665

Krushnisky, A., Mercier-Langevin, P., Ross, P.-S., Goutier, J., McNicoll, V.J., Moore, L., Pilote, C., and Bernier, C., 2018. Controls on the distribution, style, composition and timing of the gold-bearing mineralized zones of the Horne 5 deposit, Abitibi greenstone belt, Quebec; *in* Targeted Geoscience Initiative: 2017 report of activities, volume 1, (ed.) N. Rogers; Geological Survey of Canada, Open File 8358, p. 95–98. doi:10.4095/306439

Krushnisky, A., Mercier-Langevin, P., Ross, P.-S., Goutier, J., Pilote, C., and Bernier, C., 2020. Geology and gold enrichment at the Horne 5 Archean volcanogenic massive sulphide deposit, Abitibi greenstone belt, Quebec: A synthesis; *in* Targeted Geoscience Initiative 5: Contributions to the Understanding of Canadian Gold Systems, (ed.) P. Mercier-Langevin, C.J.M. Lawley, and S. Castonguay; Geological Survey of Canada, Open File 8712, p. 31–44. doi:10.4095/323663

Lafrance, B., 2015. Structural and lithological controls on gold mineralization at the Cheminis mine: Implications for the formation of gold deposits along the Cadillac – Larder Lake deformation zone, Ontario; in Targeted Geoscience Initiative 4: Contributions to the Understanding of Precambrian Lode Gold Deposits and Implications for Exploration, (ed.) B. Dubé and P. Mercier-Langevin; Geological Survey of Canada, Open File 7852, p. 49–54. doi:10.4095/296624

Lauzon, M.-C., Mercier-Langevin, P., Beaudoin, G., Côté-Mantha, O., Simard, M., Valette, M., and De Souza, S., 2017. Mineralogy and geochemistry of the Whale Tail zone, Amaruq gold project, Nunavut; Geological Survey of Canada, Scientific Presentation 61, 1 sheet. doi: 10.4095/300659

Lauzon, M.-C., Mercier-Langevin, P., Valette, M., Beaudoin, G., De Souza, S., Côté-Mantha, O., and Simard, M., 2020. Ore mineralogy and mineral chemistry of the Whale Tail zone, Amaruq gold deposit, Nunavut; *in* Targeted Geoscience Initiative 5: Contributions to the Understanding of Canadian Gold Systems, (ed.) P. Mercier-Langevin, C.J.M. Lawley, and S. Castonguay; Geological Survey of Canada, Open File 8712, p. 267–279. doi:10.4095/326044

Lawley, C.J.M. and Kjarsgaard, B.A., 2020. Bottom-up mineral exploration: Ore-element upgrading in the upper mantle and tools for its discovery; *in* Targeted Geoscience Initiative 5: Contributions to the Understanding of Canadian Gold Systems, (ed.) P. Mercier-Langevin, C.J.M. Lawley, and S. Castonguay; Geological Survey of Canada, Open File 8712, p. 157–164. doi:10.4095/323674

Lawley, C.J.M., Creaser, R.A., Jackson, S., Yang, Z., Davis, B., Dubé, B., Mercier-Langevin, P., Pehrsson, S., and Vaillancourt, D., 2015. Protracted Paleoproterozoic gold history at the Archean BIF-hosted Meliadine Gold District, Nunavut; Geological Survey of Canada, Open File 7743, 23 p. doi:10.4095/295629

Lawley, C.J.M., Dubé, B., Mercier-Langevin, P., and Vaillancourt, D., 2015. Mapping hydrothermal footprints: case studies from the Meliadine Gold District, Nunavut; Geological Survey of Canada, Open File 7744, 22 p. doi:10.4095/295920

Lawley, C.J.M., Dubé, B., Mercier-Langevin, P., Kjarsgaard, B.A., and Knight, R.D., 2015. Whole-rock lithogeochemistry and pXRF data from the Meliadine gold district, Nunavut, Canada; Geological Survey of Canada, Open File 7711, 11 p. doi:10.4095/296223

Lawley, C.J.M., Dubé, B., Mercier-Langevin, P., McNicoll, V.J., Creaser, R.A., Pehrsson, S.J., Castonguay, S., Blais, J.-C., Simard, M., Davis, W.J., and Jackson, S.E., 2015. Setting, age, and hydrothermal footprint of the emerging Meliadine gold district, Nunavut; *in* Targeted Geoscience Initiative 4: Contributions to the Understanding of Precambrian Lode Gold Deposits and Implications for Exploration, (ed.) B. Dubé and P. Mercier-Langevin; Geological Survey of Canada, Open File 7852, p. 99–111. doi:10.4095/296624

Lawley, C.J.M., McNicoll, V.J., Creaser, R.A., Dubé, B., Mercier-Langevin, P., Pehrsson, S.J., and Vaillancourt, D., 2015. Unravelling the Archean to Proterozoic history at the Meliadine Gold District, Nunavut, Canada; Geological Survey of Canada, Open File 7884, 1 sheet. doi:10.4095/297045

Lawley, C.J.M., Jackson, S.E., Yang, Z., Davis, W.J., Creaser, R.A., Mercier-Langevin, P., and Dubé, B., 2017. Tracing gold mobility using in situ Pb isotope geochemistry of early and remobilized sulphide minerals, Meliadine gold district, Nunavut; Geological Survey of Canada, Scientific Presentation 51, 39 p., 1 .pptx file.

Lawley, C.J.M., Kjarsgaard, B.A., Zagorevski, A., Jackson, S.E., Yang, Z., and Mercier-Langevin, P., 2017. Mantle metal mobility; in Targeted Geoscience Initiative: 2016 report of activities, (ed.) N. Rogers; Geological Survey of Canada, Open File 8199, p. 23–25. doi:10.4095/299581

Lawley, C.J.M., McNicoll, V.J., Davis, W.J., Jackson, S.E., Yang, Z., and Mercier-Langevin, P., 2017. Paleoproterozoic gold and its tectonic triggers and traps; in Targeted Geoscience Initiative: 2016 report of activities, (ed.) N. Rogers; Geological Survey of Canada, Open File 8199, p. 33–34. doi:10.4095/299584

Lawley, C.J.M., Jackson, S.E., Petts, D.C., Savard, D., Zagorevski, A., Pearson, D.G., Tschirhart, V., and Kjarsgaard, B., 2018. Precious metal mobility during serpentinization-driven redox reactions; Geological Survey of Canada, Open File 8506, 1 sheet. doi:10.4095/315041

Lawley, C.J.M., Kjarsgaard, B.A., Jackson, S.E., Yang, Z., and Petts, D., 2018. Olivine and clinopyroxene mantle xenocryst geochemistry from the Kirkland Lake kimberlite field, Ontario; Geological Survey of Canada, Open File 8376, 9 p. doi:10.4095/308048

Lawley, C.J.M., Kjarsgaard, B.A., Jackson, S.E., Yang, Z., Petts, D.C., and Roots, E., 2018. Mapping the ore element signature of the Abitibi Greenstone Belt cratonic mantle, Ontario; Geological Survey of Canada, Open File 8387, 1 sheet. doi:10.4095/308417

Lawley, C.J.M., Kjarsgaard, B.A., Jackson, S.E, Yang, Z., Petts, D., and Roots, E., 2018. Olivine and clinopyroxene mantle xenocryst geochemistry from the Kirkland Lake kimberlite field, Ontario; Geological Survey of Canada, Open File 8387, 1 sheet. doi:10.4095/308417

Lawley, C.J.M., Kjarsgaard, B.A., Zagorevski, A., Pearson, G., Waterton, P., Savard, D., Jackson, S.E., Yang, Z., Zhang, S., and Tschirhart, V., 2018. Preliminary geochemical results on mantle metal mobility; *in* Targeted Geoscience Initiative: 2017 report of activities, volume 1, (ed.) N. Rogers; Geological Survey of Canada, Open File 8358, p. 127–131. doi:10.4095/306445

Lawley, C.J.M., Schneider, D., Yang, E., Davis, W.J., Jackson, S.E., Yang, Z., Zhang, S., and Selby, D., 2018. Age relationships and preliminary U-Pb zircon geochronology results from the Lynn Lake Greenstone Belt; *in* Targeted Geoscience Initiative: 2017 report of activities, volume I, (ed.) N. Rogers; Geological Survey of Canada, Open File 8358, p. 133–137. doi:10.4095/306459

Lawley, C.J.M., Davis, W.J., Jackson, S.E., Petts, D.C., Yang, E., Zhang, S., Selby, D., O'Connor, A.R., and Schneider, D.A., 2019. Paleoproterozoic gold and its tectonic triggers and traps; *in* Targeted Geoscience Initiative: 2018 report of activities, (ed.) N. Rogers; Geological Survey of Canada, Open File 8549, p. 71–75. doi:10.4095/313641

Lawley, C.J.M., Jackson, S.E., Petts, D.C., Savard, D., Pearson, D.G., Zhang, S., Zagorevski, A. and Kjarsgaard, B.A., 2019. Mantle metal mobility: preliminary gold and platinum group element geochemical results; *in* Targeted Geoscience Initiative: 2018 report of activities, (ed.) N. Rogers; Geological Survey of Canada, Open File 8549, p. 43–48. doi:10.4095/313635

Lawley, C.J.M., Selby, D., Davis, W.J., Yang, E., Zhang, S., Jackson, S.E., Petts, D.C., O'Connor, A.R., and Schneider, D.A., 2020. Paleoproterozoic gold and its tectonic triggers and traps: Implications from Re-Os sulphide and U-Pb detrital zircon geochronology, Lynn Lake, Manitoba; *in* Targeted Geoscience Initiative 5: Contributions to the Understanding of Canadian Gold Systems, (ed.) P. Mercier-Langevin, C.J.M. Lawley, and S. Castonguay; Geological Survey of Canada, Open File 8712, p. 211–222. doi:10.4095/326033

Mercier-Langevin, P., Hannington, M.D., Dubé, B., Piercey, S.J., Peter, J.M., and Pehrsson, S.J., 2015. Precious metal enrichment processes in volcanogenic massive sulphide deposits — A summary of key features, with an emphasis on TIGI-4 research contributions; *in* Targeted Geoscience Initiative 4: Contributions to the Understanding of Volcanogenic Massive Sulphide Deposit Genesis and Exploration Methods Development, (ed.) J.M. Peter and P. Mercier-Langevin; Geological Survey of Canada, Open File 7853, p. 117–130. doi:10.4095/296540

Mercier-Langevin, P., Dubé, B., Castonguay, S., McNicoll, V., Pinet, N., Lawley, C., Bleeker, W., Bécu, V., Jackson, S., Davis, B., Enkin, R., Goutier, J., Préfontaine, S., Robichaud, L., Pilote, P., and Roy, P., 2017. Gold through space and time at the Archean: *in* Targeted Geoscience Initiative: 2016 report of activities, (ed.) N. Rogers; Geological Survey of Canada, Open File 8199, p. 17–21. doi:10.4095/299575

Mercier-Langevin, P., Dubé, B., Pitre, D., Bégin, J.-F., Laberge, A., and Burke, L., 2017. (Day 4) Au-rich VMS deposits of the Doyon-Bousquet-LaRonde mining camp – The LaRonde Penna mine; Chapter 7 *in* Precious- and Base-Metal Deposits of the southern Abitibi Greenstone Belt, Superior Province, Canada: A field trip to the 14th Biennial Society for Geology Applied to Mineral Deposits meeting, (ed.) P. Mercier-Langevin, J. Goutier, and B. Dubé; Geological Survey of Canada, Open File 8317, p. 49–54. doi:10.4095/306258

Mercier-Langevin, P., Goutier, J., and Dubé, B. (ed.), 2017. Precious and base metal deposits of the southern Abitibi greenstone belt, Superior Province, Canada: A field trip to the 14th Biennial Society for Geology Applied to Mineral Deposits meeting; Geological Survey of Canada, Open File 8317, 86 p. doi:10.4095/306250

Mercier-Langevin, P., Janvier, V., McNicoll, V., Castonguay, S., Dupuis, C., Dubé, B., de Chavigny, B., and Côté-Mantha, O., 2017. Géologie du gisement d'or Vault et implications pour l'exploration aurifère dans les ceintures de roches vertes précambriennes; Geological Survey of Canada, Scientific Presentation 64, 1 sheet. doi:10.4095/300661

Mercier-Langevin, P., Rogers, N., Dubé, B., Bleeker, W., Castonguay, S., McNicoll, V.J., Chapman, J.B., Lawley, C.J.M., Bellefleur, G., Houlé, M.G., Pinet, N., Jackson, S., Davis, B., Bécu, V., Peter, J.M., Paradis, S., Potter, E.G., Bjerkelund, C., Villeneuve, M.E., and Evans, R., 2017, Targeted Geoscience Initiative: 2016 Report of Activities – an overview: *in* Targeted Geoscience Initiative: 2016 report of activities, (ed.) N. Rogers; Geological Survey of Canada, Open File 8199, p. 7–16. doi:10.4095/299574

Mercier-Langevin, P., Valette, M., De Souza, S., McNicoll, V.J., Grondin-LeBlanc, P., Creaser, R.A., Côté-Mantha, O., Simard, M., and Malo, M., 2017. Lithologic and tectonic controls on Paleoproterozoic BIF-hosted/associated gold; *in* Targeted Geoscience Initiative: 2016 report of activities, (ed.) N. Rogers; Geological Survey of Canada, Open File 8199, p. 39–42. doi:10.4095/299586

Mercier-Langevin, P., Valette, M., De Souza, S., Creaser, R.A., McNicoll, V.J., Grondin-Leblanc, P., St.Pierre, B., Lauzon, M.-C., Malo, M., Côté-Mantha, O., and Simard, M., 2018. Lithologic controls on Paleoproterozoic BIF-hosted/associated gold: Overview of Re-Os geochronology and Pb isotopes preliminary results; *in* Targeted Geoscience Initiative: 2017 report of activities, volume 1, (ed.) N. Rogers; Geological Survey of Canada, Open File 8358, p. 147–152. doi:10.4095/306466

Mercier-Langevin, P., Lawley, C.J.M., Castonguay, S., Dubé, B., Bleeker, W., Pinet, N., Bécu, B., Pilote, J.-L., Jackson, S.E., Wodicka, N., Honsberger, I.W., Davis, W.J., Petts, D.C., Yang, Z., Jautzy, J., and Lauzière, K., 2020. Targeted Geoscience Initiative 5, Gold Project: A summary of contributions to the understanding of Canadian gold systems; *in* Targeted Geoscience Initiative 5: Contributions to the Understanding of Canadian Gold Systems, (ed.) P. Mercier-Langevin, C.J.M. Lawley, and S. Castonguay; Geological Survey of Canada, Open File 8712, p. 1–30. doi:10.4095/ 323662

Ootes, L., Castonguay, S., Friedman, R., Devine, F., and Simmonds, R., 2017. Geological fieldwork 2017: A summary of field activities and current research; *in* Geological Fieldwork 2017; British Columbia Ministry of Energy, Mines and Petroleum Resources, British Columbia Geological Survey, Paper 2018-1, p. 67–81.

Ootes, L., Castonguay, S., Friedman, R., and Devine, F., 2019. Superimposed auriferous structural events along the Llewellyn-Tally Ho deformation corridor in southern Yukon and northwest British Columbia; *in* Targeted Geoscience Initiative: 2018 report of activities, (ed.) N. Rogers; Geological Survey of Canada, Open File 8549, p. 49–58. doi:10.4095/313636

Oswald, W., Castonguay, S., Dubé, B., Malo, M., Mercier-Langevin, P. and Biczok, J., 2015. New insights on the geological and structural settings of the Musselwhite banded iron formation-hosted gold deposit, North Caribou greenstone belt, Superior Province, Ontario; Geological Survey of Canada, Current Research 2015-3, 19 p. doi:10.4095/295570

Oswald, W., Castonguay, S., Dubé, B., McNicoll, V., Biczok, J., Malo, M., and Mercier-Langevin, P., 2015. Geological setting of the world-class Musselwhite gold Mine, Superior Province, northwestern Ontario, and implications for exploration; *in* Targeted Geoscience Initiative 4: Contributions to the Understanding of Precambrian Lode Gold Deposits and Implications for Exploration, (ed.) B. Dubé and P. Mercier-Langevin; Geological Survey of Canada, Open File 7852, p. 69–84. doi:10.4095/296624

Pelletier, M., Mercier-Langevin, P., Dubé, B., Crick, D., McNicoll, V., Jackson, S., and Beakhouse, G.P., 2015. The Rainy River "atypical" Archean Au deposit, western Wabigoon Subprovince, Ontario; *in* Targeted Geoscience Initiative 4: Contributions to the Understanding of Precambrian Lode Gold Deposits and Implications for Exploration, (ed.) B. Dubé and P. Mercier-Langevin; Geological Survey of Canada, Open File 7852, p. 193–207. doi:10.4095/296624

Pelletier, M., Mercier-Langevin, P., Dubé, B., Bécu, V., Lauzière, K., and Richer-Laflèche, M., 2016. Whole-rock lithogeochemistry of the Archean Rainy River gold deposit, western Wabigoon, Ontario; Geological Survey of Canada, Open File 8048, 1 .zip file. doi:10.4095/ 299356

Pilote, J.-L., Piercey, S.J., and Mercier-Langevin, P., 2015. Volcanic architecture and alteration assemblages of the Ming Cu-Au-(Zn-Ag) VMS deposit, Baie Verte, Newfoundland and Labrador: Implications for Au-enrichment processes and exploration; *in* Targeted Geoscience Initiative 4: Contributions to the Understanding of Volcanogenic Massive Sulphide Deposit Genesis and Exploration Methods Development, (ed.) J.M. Peter and P. Mercier-Langevin; Geological Survey of Canada, Open File 7853, p. 197–210. doi:10.4095/ 296540

Pilote, J.-L., Piercey, S.J., and Mercier-Langevin, P., 2016. Geological environment and formational controls of auriferous massive sulfide deposit: An example from the Cambro-Ordovician Cu-Au Ming VMS deposit in the Newfoundland Appalachians; Geological Survey of Canada, Open File 7731, 1 sheet. doi:10.4095/298770

Pilote, J.-L., Jackson, S.E., Mercier-Langevin, P., Dubé, B., and Rhys, D., 2019. Characteristics of diagenetic and epigenetic sulphides in deformed and metamorphosed Archean carbonaceous metasedimentary rocks of the Timmins-Matheson corridor: establishing a framework for fingerprinting ore-forming processes in shear zone-hosted orogenic gold systems; *in* Targeted Geoscience Initiative: 2018 report of activities, (ed.) N. Rogers; Geological Survey of Canada, Open File 8549, p. 33–41. doi:10.4095/313632

Pilote, J.-L., Jackson, W.E., Mercier-Langevin, P., Dubé, B., Lawley, C.J.M., Petts, D.C., Yang, Z., van Hees, E., and Rhys, D., 2020. Fingerprinting ore processes in orogenic auriferous systems: Insights into metallogenic and exploration implications from argillite-hosted iron sulphide nodules from the Timmins-Matheson gold corridor; *in* Targeted Geoscience Initiative 5: Contributions to the Understanding of Canadian Gold Systems, (ed.) P. Mercier-Langevin, C.J.M. Lawley, and S. Castonguay; Geological Survey of Canada, Open File 8712, p. 165–178. doi:10.4095/323675

Pilote, J.-L., Mercier-Langevin, P., Jackson, S.E., Dubé, B., Yang, Z., Lawley, C.J.M., Petts, D.C., Layne, G.D., and Piercey, S.J., 2020. Interrogating the composition and genesis of argillite-hosted pyrite nodules at the LaRonde Penna gold-rich volcanogenic massive sulphide deposit, Abitibi, Quebec: Insights into metallogenic implications; *in* Targeted Geoscience Initiative 5: Contributions to the Understanding of Canadian Gold Systems, (ed.) P. Mercier-Langevin, C.J.M. Lawley, and S. Castonguay; Geological Survey of Canada, Open File 8712, p. 75–91. doi:10.4095/323666

Pinet, N. and Sack, P.J., 2019. Macroscopic control on Carlin-type gold mineralization in north-central Yukon; *in* Targeted Geoscience Initiative: 2018 report of activities, (ed.) N. Rogers; Geological Survey of Canada, Open File 8549, p. 89–103. doi:10.4095/313644

Pinet, N., Mercier-Langevin, P., Dubé, B., Colpron, M., Lane, J., and Asselin, E., 2017. Lithotectonic controls on the genesis and distribution of carbonate replacement-type ("Carlin-type") gold zones, east-central, Yukon; *in* Targeted Geoscience Initiative: 2016 report of activities, (ed.) N. Rogers; Geological Survey of Canada, Open File 8199, p. 43–45. doi:10.4095/299587

Pinet, N., Sack, P.J., Mercier-Langevin, P., Lavoie, D., Dubé, B., Lane, J., and Brake, V., 2018. Breccia styles and controls on carbonate replacement-type ("Carlin-type") gold zones, Rackla belt, east-central Yukon; in Targeted Geoscience Initiative: 2017 report of activities, volume 1, (ed.) N. Rogers; Geological Survey of Canada, Open File 8358, p. 163–168. doi:10.4095/306469

Pinet, N., Sack, P., Mercier-Langevin, P., Colpron, M., Lavoie, D., Dubé, B., and Brake, V.I., 2020. Neoproterozoic-hosted Carlin-type mineralization in central Yukon, part 1: Regional- to prospect-scale geological controls; *in* Targeted Geoscience Initiative 5: Contributions to the Understanding of Canadian Gold Systems, (ed.) P. Mercier-Langevin, C.J.M. Lawley, and S. Castonguay; Geological Survey of Canada, Open File 8712, p. 281–297. doi:10.4095/326045

Pinet, N., Sack, P., Mercier-Langevin, P., Davis, W.J., Lavoie, D., Haeri-Ardakani, O., Komaromi, B.A., Dubé, B., Cline, J.S., Petts, D.C., Jautzy, J., Jackson, S.E., Percival. J.B., Savard, M.M., and Brake, V.I., 2020. Neoproterozoic-hosted Carlin-type mineralization in central Yukon part 2: Mineralization; *in* Targeted Geoscience Initiative 5: Contributions to the Understanding of Canadian Gold Systems, (ed.) P. Mercier-Langevin, C.J.M. Lawley, and S. Castonguay; Geological Survey of Canada, Open File 8712, p. 299–314. doi:10.4095/ 326047

St.Pierre, B., Mercier-Langevin, P., Simard, M., Côté-Mantha, O., Malo, M., and Servelle, G., 2018. Structural and lithologic controls on the nature and distribution of gold in the BIF-associated 1150 and 1250 lode series at Tiriganiaq, Meliadine district, Rankin Inlet greenstone belt, Nunavut; *in* Targeted Geoscience Initiative: 2017 report of activities, volume I, (ed.) N. Rogers; Geological Survey of Canada, Open File 8358, p. 157–161. doi:10.4095/306468

St.Pierre, B., Mercier-Langevin, P., Simard, M., Côté-Mantha, O., Malo, M., and Servelle, G., 2019. Structural and lithological controls on the nature and distribution of gold at the Tiriganiaq deposit, Meliadine district, Rankin Inlet greenstone belt, Nunavut; *in* Targeted Geoscience Initiative: 2018 report of activities, (ed.) N. Rogers; Geological Survey of Canada, Open File 8549, p. 77–82. doi:10.4095/313642

St.Pierre, B., Mercier-Langevin, P., Blais, J.-C., Servelle, G., Simard, M., Côté-Mantha, O., and Malo, M., 2020. Structural controls and relative timing of gold mineralization of the banded iron formation-associated Tiriganiaq deposit, Meliadine district, Rankin Inlet greenstone belt, Nunavut; *in* Targeted Geoscience Initiative 5: Contributions to the Understanding of Canadian Gold Systems, (ed.) P. Mercier-Langevin, C.J.M. Lawley, and S. Castonguay; Geological Survey of Canada, Open File 8712, p. 237–250. doi:10.4095/326041

Tóth, Z., Lafrance, B., Dubé, B., McNicoll, V., Mercier-langevin, P., and Creaser, R.A., 2015. Banded Iron formation-hosted gold mineralization in the Geraldton area, Northwestern Ontario: structural setting, mineralogical characteristics and geochronology; *in* Targeted Geoscience Initiative 4: Contributions to the Understanding of Precambrian Lode Gold Deposits and Implications for Exploration, (ed.) B. Dubé and P. Mercier-Langevin; Geological Survey of Canada, Open File 7852, p. 85–97. doi:10.4095/296624

Tóth, Z., Lafrance, B., Dubé, B., Mercier-Langevin, P., and McNicoll, V.J., 2015. Structural setting, mineralogical characteristics and geochemical footprints of banded-iron-formation-hosted gold mineralization in the Geraldton area, Ontario; Geological Survey of Canada, Open File 7667, 1 sheet. doi:10.4095/295526

Valette, M., De Souza, S., Mercier-Langevin, P., Côté-Mantha, O., Simard, M., McNicoll, V., and Barbe, P., 2017. Geology of the 130 t (4.2 Moz) Au, banded iron-formation-hosted Amaruq project, Nunavut; Geological Survey of Canada, Scientific Presentation 60, 1 sheet. doi:10.4095/300658

Valette, M., De Souza, S., Mercier-Langevin, P., McNicoll, V.J., Grondin-LeBlanc, P., Côté-Mantha, O., Simard, M., and Malo, M., 2018. Lithological, hydrothermal, structural and metamorphic controls on the style, geometry and distribution of the auriferous zones at Amaruq, Churchill Province, Nunavut; *in* Targeted Geoscience Initiative: 2017 report of activities, volume 1, (ed.) N. Rogers; Geological Survey of Canada, Open File 8358, p. 153–156. doi:10.4095/306467

Valette, M., De Souza, S., Mercier-Langevin, P., McNicoll, V.J., Wodicka, N., Creaser, R.A., Cote-Mantha, O., and Simard, M., 2019. Geological setting of the 5.2 Moz Au Amaruq banded iron formation-hosted gold deposit, Churchill Province, Nunavut; *in* Targeted Geoscience Initiative: 2018 report of activities, (ed.) N. Rogers; Geological Survey of Canada, Open File 8549, p. 83–87. doi:10.4095/313643

Valette, M., De Souza. S., Mercier-Langevin, P., Côté-Mantha, O., Simard, M., Wodicka, N., McNicoll, V.J., and Barbe, P., 2020. Lithological and tectonic controls on banded iron formation-associated gold at the Amaruq deposit, Churchill Province, Nunavut, and implications for exploration; *in* Targeted Geoscience Initiative 5: Contributions to the Understanding of Canadian Gold Systems, (ed.) P. Mercier-Langevin, C.J.M. Lawley, and

S. Castonguay; Geological Survey of Canada, Open File 8712, p. 251–266. doi:10.4095/ 326042

Yang, X.M. and Lawley, C.J.M., 2018. Tectonic setting of the Gordon gold deposit, Lynn Lake greenstone belt, northwestern Manitoba (parts of NTS 64C16): Evidence from lithogeochemistry, Nd isotopes and U-Pb geochronology; *in* Report of Activities 2018; Manitoba Growth, Enterprise and Trade, Manitoba Geological Survey, p. 89–109.

Yergeau, D., Mercier-Langevin, P., Dubé, B., Malo, M., McNicoll, V., Jackson, S., Savoie, A., and La Rochelle, F., 2015. The Archean Westwood Au deposit, southern Abitibi: telescoped Au-rich VMS and intrusion-related Au systems; *in* Targeted Geoscience Initiative 4: Contributions to the Understanding of Precambrian Lode Gold Deposits and Implications for Exploration, (ed.) B. Dubé and P. Mercier-Langevin; Geological Survey of Canada, Open File 7852, p. 177–191. doi:10.4095/296624

Yergeau, D., Mercier-Langevin, P., Dubé, B., Malo, M., Bécu, V., and Lauzière, K., 2019. Whole-rock lithogeochemistry of the Archean Westwood deposit, southern Abitibi, Québec; Geological Survey of Canada, Open File 8171, 1 .zip file. doi:10.4095/321380

Appendix 3
Theses related to the TGI-5 Gold Project (2015–2020) and legacies of the TGI-4 Lode Gold Project (2010–2015)

Beauchamp, A.-M., 2018. L'indice Mustang : géologie et altération d'une minéralisation aurifère mise en place dans les turbidites de la ceinture de la Basse-Eastmain, Eeyou Itschee Baie-James; M.Sc. thesis, Institut national de la recherche scientifique – Centre Eau Terre Environnement, Québec, Quebec, 360 p.

Boily-Auclair, E., 2017. Nature et style de l'altération hydrothermale associée aux minéralisations aurifères du projet LaRonde Zone 5 (LZ-5), Abitibi, Québec; B.Sc. thesis, Université Laval, Québec, Quebec, 69 p.

Boily-Auclair, E., in prep. Contrôles lithologiques et structuraux sur la nature, le style et la géométrie des zones aurifères de la Zone 5 du complexe minier LaRonde, Abitibi, Québec; M. Sc. thesis, Institut national de la recherche scientifique – Centre Eau Terre Environnement, Québec, Quebec.

Boulerice, A., 2016. Volcanology of the Lemoine Member of the Waconichi Formation, Abitibi Subprovince, Chibougamau, Quebec; M.Sc. thesis, Institut national de la recherche scientifique – Centre Eau Terre Environnement, Québec, Quebec, 193 p.

Caté, A., 2017. Geology of the Paleoproterozoic Zn-Cu-Au lalor volcanogenic massive sulphide deposit and its gold-rich lenses, Snow Lake, Manitoba; Ph.D. thesis, Institut national de la recherche scientifique – Centre Eau Terre Environnement, Québec, Quebec, 384 p.

Ciufo, T.J., 2019. Hydrothermal alteration and exploration vectors at the Island Gold deposit, Michipicoten greenstone belt, Wawa, Ontario; M.Sc. thesis, University of Waterloo, Waterloo, Ontario, 510 p.

Dubé, J., 2016. Caractérisation de la distribution de l'or à l'intérieur de la lentille 20 Nord dans le secteur LaRonde Extension à la mine LaRonde Penna, Abitibi, Québec; B.Sc. thesis, Université Laval, Québec, Quebec, 115 p.

Duff, S., 2016. Ore types of the auriferous Lalor VMS deposit, Snow Lake, Manitoba: implications for genesis and post-depositional processes; M.Sc. thesis, University of Ottawa, Ottawa, Ontario, 123 p.

Fayard, Q., in prep. Contrôles primaires et secondaires principaux sur la nature et la distribution de l'or et de l'argent dans les zones minéralisées du projet B26, complexe volcanique de Brouillan, Abitibi, Québec; M.Sc. thesis, Université du Québec à Chicoutimi, Chicoutimi, Quebec.

Fontaine, A., 2019. Géologie des minéralisations aurifères de la mine Éléonore, Eeyou Istchee Baie-James, province du Supérieur, Québec, Canada; Ph.D. thesis, Institut national de la recherche scientifique – Centre Eau Terre Environnement, Québec, Quebec, 526 p.

Gourcerol, B., 2016. Characterization of banded iron formations associated with gold mineralization primary geochemical signatures and exploration implications; Ph.D. thesis, Laurentian University, Sudbury, Ontario, 370 p.

Janvier, V. 2016. Géologie du gisement d'or encaissé dans des formations de fer rubanées Meadowbank, Nunavut, Canada; Ph.D. thesis, Institut national de la recherche scientifique – Centre Eau Terre Environnement, Québec, Quebec, 472 p.

Jellicoe, K.M., 2019. Structural controls and deformation history of the orogenic Island Gold deposit, Michipicoten greenstone belt, Ontario; M.Sc. thesis, University of Waterloo, Waterloo, Ontario, 84 p.

Katz, L.R., 2016. Geology of the Archean Côté Gold Au(-Cu) intrusion-related deposit, Swayze Greenstone Belt, Ontario; Ph.D. thesis, Laurentian University, Sudbury, Ontario, 347 p.

Krushnisky, A., 2018. Controls on gold enrichment at the Horne 5 Archean VMS deposit, Abitibi greenstone belt, Québec; M.Sc. thesis, Institut national de la recherche scientifique – Centre Eau Terre Environnement, Québec, Quebec, 198 p.

Lauzon, M.-C., 2017. Empreinte minéralogique et géochimique des minéralisations aurifères de la zone Whale Tail du projet Amaruq; B.Sc. thesis, Université Laval, Québec, Quebec, 48 p.

O'Connor, A.R., in prep. Thermochronology of the Lynn Lake greenstone belt, Manitoba; M.Sc. thesis, University of Ottawa, Ottawa, Ontario.

Oswald, W., 2018. Geology of the Musselwhite banded iron formation-hosted gold deposit, Superior Province, Ontario, Canada; Ph.D. thesis, Institut national de la recherche scientifique – Centre Eau Terre Environnement, Québec, Quebec, 475 p.

Pelletier, M., 2016. The Rainy River gold deposit, Wabigoon Subprovince, Western Ontario: style, geometry, timing and structural controls on ore distribution and grades; M.Sc. thesis, Institut national de la recherche scientifique – Centre Eau Terre Environnement, Québec, Quebec, 364 p.

Appendix 3: Theses related to the TGI-5 Gold Project (2015–2020) and legacies of the TGI-4 Lode Gold Project (2010–2015); *in* Targeted Geoscience Initiative 5: Contributions to the Understanding of Canadian Gold Systems, (ed.) P. Mercier-Langevin, C.J.M. Lawley, and S. Castonguay; Geological Survey of Canada, Open File 8712, p. 327–328.

Pilote, J.-L. 2018. Geology, structure, petrogenesis, and hydrothermal alteration reconstruction of the Ming volcanogenic massive sulphide deposit, Baie Verte Peninsula, Newfoundland, Canada; Ph.D. thesis, Memorial University of Newfoundland, St-John's, Newfoundland and Labrador, 496 p.

St.Pierre, B., in prep. Structural and lithological controls on the nature and distribution of gold in the BIF-associated 1150 and 1250 lode series at Tiriganiaq, Meliadine district, Rankin Inlet greenstone belt, Nunavut; M.Sc. thesis, Institut national de la recherche scientifique – Centre Eau Terre Environnement, Québec, Quebec.

Sterckx, S., 2018. Géochimie des roches volcaniques archéennes du Groupe de Blake River, ceinture de roches vertes de l'Abitibi, Québec; M.Sc. thesis, Institut national de la recherche scientifique – Centre Eau Terre Environnement, Québec, Quebec, 209 p.

Tóth, Z., 2019. The geology of the Beardmore-Geraldton belt, Ontario, Canada: geochronology, tectonic evolution and gold mineralization; Ph.D. thesis, Laurentian University, Sudbury, Ontario, 303 p.

Valette, M., in prep. Contexte géologique, évolution tectono-métamorphique et activité hydrothermale du secteur Amaruq: implications pour la genèse des minéralisations aurifères de l'ouest de la Province de Churchill, Nunavut; Ph.D. thesis, Université du Québec à Montréal, Montréal, Quebec.

Veglio, C., in prep. Ore-forming element signature of the Slave cratonic mantle; M.Sc. thesis, University of Alberta, Edmonton, Alberta.

Watts, J., in prep. Element mapping of gold veins and geochemical vectoring with handheld LIBS, Lynn Lake, Manitoba; M.Sc. thesis, University of Windsor, Windsor, Ontario.